1 **Inter-comparison of online and offline methods for measuring ambient heavy and trace elements**
2 **and water-soluble inorganic ions (NO$_3^-$, SO$_4^{2-}$, NH$_4^+$ and Cl$^-$) in PM$_{2.5}$ over a heavily polluted**
3 **megacity, Delhi**

4 Himadri Sekhar Bhowmik[1], Ashutosh Shukla[1], Vipul Lalchandani[1], Jay Dave[2], Neeraj Rastogi[2], Mayank
5 Kumar[3], Vikram Singh[4], and Sachchida Nand Tripathi[1*]

6 [1] Department of Civil Engineering, Indian Institute of Technology Kanpur, Kanpur, India

7 [1*] Department of Civil Engineering and Centre for Environmental Science and Engineering, Indian
8 Institute of Technology Kanpur, Kanpur, India

9 [2] Geosciences Division, Physical Research Laboratory, Ahmedabad, India

10 [3]Department of Mechanical Engineering, Indian Institute of Technology Delhi, New Delhi, India

11 [4]Department of Chemical Engineering, Indian Institute of Technology Delhi, New Delhi, India

12 *Correspondence to:* S. N. Tripathi (snt@iitk.ac.in)

15 **Abstract**

16 Characterizing the chemical composition of ambient particulate matter (PM) provides valuable
17 information on the concentration of secondary species, toxic metals and assists in the validation of
18 abatement techniques. The chemical components of PM can be measured by sampling on filters and
19 analysing them in the laboratory or using real-time measurements of the species. It is important for the
20 accuracy of the PM monitoring networks that measurements from the offline and online methods are
21 comparable and biases are known. The concentrations of water-soluble inorganic ions (NO$_3^-$, SO$_4^{2-}$, NH$_4^+$
22 and Cl$^-$) in PM$_{2.5}$ measured from the 24 hrs filter samples using ion chromatography (IC) were compared
23 with the online measurements of inorganics from aerosol mass spectrometer (AMS) with a frequency of 2
24 mins. Also, the concentrations of heavy and trace elements determined from the 24 hrs filter samples
25 using inductively coupled plasma mass spectroscopy (ICP-MS) were compared with the online
26 measurements of half-hourly heavy and trace metal's concentrations from Xact 625i ambient metal mass
27 monitor. The comparison was performed over two seasons (summer and winter) and at two sites (Indian
28 Institute of Technology, Delhi and Indian Institute of Tropical Meteorology, Delhi) which are located in

29 Delhi, NCR, India, one of the heavily polluted urban areas in the world. Collocated deployments of the

30 instruments helped to quantify the differences between online and offline measurements and evaluate the

31 possible reasons for positive and negative biases. The slopes for SO_4^{2-} and NH_4^+ were closer to 1:1 line

32 during winter and decreased during summer at both sites. The higher concentrations on the filters were

33 due to the formation of particulate $(NH_4)_2SO_4$. Filter-based NO_3^- measurements were lower than online

34 NO_3^- during summer at IITD and winter at IITMD due to the volatile nature of NO_3^- from the filter

35 substrate. Offline measured Cl^- was consistently higher than AMS derived Cl^- during summer and winter

36 at both sites. Based on their comparability characteristics, elements were grouped under 3 categories. The

37 online element data were highly correlated ($R^2 > 0.8$) with the offline measurements for Al, K, Ca, Ti, Zn,

38 Mn, Fe, Ba, and Pb during summer at IITD and winter at both the sites. The higher correlation

39 coefficient demonstrated the precision of the measurements of these elements by both Xact 625i

40 and ICP-MS. Some of these elements showed higher Xact 625i elemental concentrations than ICP-MS

41 measurements by an average of 10-40% depending on the season and site. The reasons for the differences

42 in the concentration of the elements could be the distance between two inlets for the two methods, line

43 interference between two elements in Xact measurements, sampling strategy, variable concentrations of

44 elements in blank filters and digestion protocol for ICP measurements.

1. Introduction

46 The adverse effect of ambient particulate matter (PM) on human health and the role of PM in visibility

47 degradation, altering earth's radiation balance, and climate change has received global attention in the last

48 two decades (Pope et al., 2009; Hong et al., 2019; Wang et al., 2019). To gain better insight into their

49 properties, the chemical characterization of particulate matter and its source attribution is crucial. The

50 National Capital Region (NCR), which includes India's capital (New Delhi) along with some districts

51 (Gurugram, Faridabad, and Noida) of the adjoined states of Haryana, Rajasthan, and Uttar Pradesh, is one

52 of the most polluted urban areas in northern India with a population over 47 million (Bhowmik et al.,

53 2021). According to World Economic Forum, New Delhi was listed as the most polluted city globally,

54 with an annual average $PM_{2.5}$ concentration of ~140 μg m^{-3} (World Health Organisation, 2018). NCR has

55 been a specific area for researchers for the past couple of years due to its unprecedented $PM_{2.5}$ levels.

56 Various large and small scale industries, power plants, construction activities, and rapid increase in the

57 vehicle numbers (11 million in 2018) (Rai et al., 2020) are among the several causes that massively

58 reduces the air quality index (AQI) (Rai et al., 2020; Sharma & Kulshrestha, 2014). Further, the crop

59 residue burning during the month of Oct-Nov in the adjoining states of Haryana and Punjab on a larger

60 scale worsens the air quality.

For decades, the mass concentrations of major water soluble inorganic ions (WSIS) and heavy and trace metals in PM have been carried out by sampling them on filters and subsequently analysing them in laboratory. Water-soluble inorganic ions (WSIS) and heavy and trace elements from these filter samples are analyzed using ion chromatography (IC) (Bhowmik et al., 2021; Rengarajan et al., 2007; Rastogi & Sarin, 2005) and inductively coupled plasma-mass spectroscopy (ICP-MS) or inductively coupled plasma-optical emission spectroscopy (ICP-OES) (Patel et al., 2021) respectively. Usually, these filters are collected over 24 hrs interval. Traditional receptor models usually use these offline measured data of very low temporal resolution, making it challenging to characterize the short pollution episodes and dynamics of pollution sources. Further, un-denuded filter sampling can have both negative and positive artifacts due to volatile species (Lipfert, 1994; Pathak & Chan, 2005). The absorption of acidic and alkaline gases on the filter substrates, if not removed prior to sampling, can give positive artifacts and result in overestimating species concentration. Likewise, the evaporation of semi-volatile compounds (ammonium nitrate) from filter substrates can give negative biases and result in underestimating aerosol concentration and its species (Pathak & Chan, 2005; X. Zhang & Mcmurryt, 1992). The degree of artifacts can be affected by several factors, including temperature, relative humidity, type of filter substrate, the aerosol loading on the filter substrate, etc. Transient events can also lead to mismatch. To overcome the limitations of low temporal resolution and avoid the artifacts associated with offline filter sampling, methods have been developed for measuring aerosol chemical composition at a higher time resolution in the order of hours or minutes.

Aerosol Mass Spectrometer (AMS) (Canagratna et al., 2007; Jayne et al., 2000; Jimenez et al., 2003) is one kind of such instrument, which provides size-resolved chemical composition of non-refractory submicron aerosols, e.g., organics, sulphate, nitrate, ammonium, and chloride at the order of hours or even minutes. For other important components, such as calcium (main constituents of soil dust and construction activities) and potassium (tracer of biomass burning), which AMS cannot measure, Xact ambient metal mass monitor can be used. It is capable of measuring 45 elements, e.g., Al, Si, P, S, Cl, K, Ca, Ti, V, Cr, Mn, Fe, Co, Ni, Cu, Zn, Ga, Ge, As, Se, Br, Rb, Sr, Y, Zr, Nb, Mo, Pd, Ag, Cd, In, Sn, Sb, Te, I, Cs, Ba, La, Ce, Pt, Au, Hg, Tl, Pb and Bi with a frequency of every 30 mins to 4 hours. However, the high time-resolution instruments measure lower range of species concentrations with higher limit of detection (LOD) than the offline based methods (Tremper et al., 2018). Both offline and online methods have their own strength and weaknesses. Uncertainties in offline filter analysis methods have been extensively studied (Pathak & Chan, 2005; Viana et al., 2006), but the novel online methods pose new problems (Wu & Wang, 2007). For example, when the ambient concentrations are very low, online measurements are often close to the MDL values due to the short integration times (Malaguti et al., 2015).

94   Previous studies in Delhi-NCR have used low time resolution filter-based methods for chemical

95   characterization of submicron aerosols (Bhowmik et al., 2020; Nagar et al., 2017; Pant et al., 2015; S. K.

96   Sharma et al., 2016; Singhai et al., 2017). On the other hand, there are only a few studies in Delhi-NCR

97   that used high time resolution methods (HR-ToF-AMS, Q-ACSM, Xact) for characterization and source

98   apportionment of coarse and fine particulate matters (Gani et al., 2019; Lalchandani et al., 2021; Rai et

99   al., 2020, 2021; Singh et al., 2021; Tobler et al., 2020). Online and offline measurements both have their

100   advantages and limitations. For both these measurements, the quality of the data highly depends on the

101   calibration of the instruments. For Xact, the multi-element mix standard might not represent ambient

102   elemental mix if the ambient particulate matters are too low or too high in concentration, affecting the

103   collection properties of the filter (Indresand et al., 2013). For filter-based water-soluble inorganic ion and

104   metal analysis, confidence in the data depends on the calibration as well as the volatility, solubility, and

105   digestion protocol used for the extraction of water-soluble inorganic ions and elements, respectively.

106   Thus, it is vital for monitoring networks that both the offline and online measurement methods give

107   comparable results. Few published studies have compared inorganics and elements from filter-based

108   measurements and semi-continuous methods (e.g., Furger et al., 2017; Nie et al., 2010). The inter-

109   comparison in these studies is unjustified for highly polluted areas, as the specie values observed in these

110   studies are much below MDL due to very low ambient concentration of secondary species and elements.

111   It will be interesting to study the inter-comparison in highly polluted areas. To the best of our knowledge,

112   there are neither any published seasonal and temporal comparisons of inorganics from high time

113   resolution AMS measurements and filter-based measurements from ion chromatography nor any

114   comparisons of heavy and trace metals from high time resolution Xact 625 ambient metal mass monitor

115   and offline measurements from ICP-MS in the heavily polluted Delhi NCR region.

116   This study demonstrates a comparison between online and offline measurements of WSIS and heavy and

117   trace metals at two sites in Delhi NCR during summer (June-July 2019), characterized by moderate levels

118   of local pollution and winter (October-December 2019), affected by high levels of pollution from local

119   sources and regional transport of crop residue burning emissions from adjoining state of Haryana and

120   Punjab.

121   **2. Methodology**

122   **2.1. Sampling sites**

123   Delhi-NCR, a highly polluted urban area with an annual average $PM_{2.5}$ concentration of 140 μg m^{-3} and a

124   population of over 47 million, is surrounded by the Thar desert on its west and Indo-Gangetic Plain on its

125   east to south-east. The temperature is about ~35°C-48°C during summer (April-June), and winter

126   (December-February) is relatively cooler, with temperature ranges from ~2°C-15°C (Bhowmik et al.,

127   2020; Vipul Lalchandani et al., 2021; Tobler et al., 2020). The wind is mostly north-westerly during both
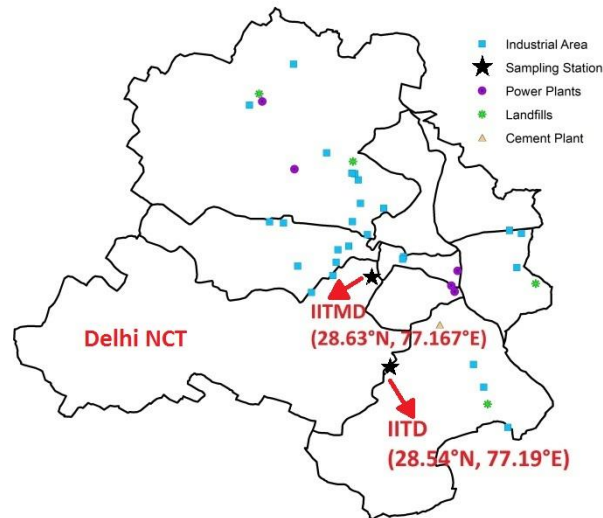
128   summer and winter.

129

130   Fig.1. Sampling sites with various emission sources like power plants, industries, landfills, etc.

131   **2.1.1. Delhi NCR site 1: IITD**

132   High volume $PM_{2.5}$ samples were collected on the rooftop of the Centre for Atmospheric Science (CAS)

133   building at the Indian Institute of Technology, Delhi (IITD) (28.54°N, 77.19°E; ~218 m amsl) about ~15

134   m above the ground level. Further, one HR-ToF-AMS and Xact ambient metal mass monitor were

135   deployed inside a temperature-controlled laboratory on the 3rd floor of the same building about ~10 m

136   above the ground level. It is an educational institute as well as residential campus having restaurants

137   nearby and very close to (<200 m) heavy traffic road. Lalchandani et al., (2021); Rai et al., (2020)

138   observed source signatures of emissions from industries, power plants, vehicles, and waste burning in this

139   site.

140   **2.1.2. Delhi NCR site 2: IITMD.**

141   Offline $PM_{2.5}$ sampling was carried out on the rooftop of the main building at the Indian Institute of

142   Tropical Meteorology Delhi (IITMD) (28.63°N, 77.167°E; ~220 m above msl) about 15 m above the

143   ground level. Moreover, HR-ToF-AMS and Xact ambient metal mass monitor were installed inside a

144 temperature-controlled laboratory on the 2nd floor of the same building at the height of ~8 m from the
145 ground level. This site is placed in the central urban area of Delhi and surrounded by Central Ridge
146 reserve forest and residential areas (Tobler et al., 2020) and around 14 km away in North West direction
147 from IITD. A recent study by Lalchandani et al. (2021) observed the site is dominated by emissions from
148 traffic, solid fuel burning, and oxidized organic aerosols. The location of the sampling sites are shown in
149 Fig. 1.

150 **2.2. Sampling details**

151 **2.2.1 Offline sampling**

152 Biweekly 24 hrs (January-May and August-September 2019) and daily 24 h (June-July and October-
153 December 2019) PM$_{2.5}$ samples were collected on quartz filter substrates (Whatman; 8×12 inches) using
154 a high-volume sampler (HVS) with a flow rate of 1.13 m^3/min. Blanks were collected in the field by
155 placing a fresh filter in the sampler while not running. A total of 64 filters (60 from IITD site during June-
156 July 2019 including 4 blanks) were collected in summer whereas, a total of 186 filters (90 from each site
157 during October-December 2019 plus 6 blanks) were collected in winter. The collected filters, including
158 field blanks, were zip-locked and stored in the freezer at each site and periodically transported to CESE
159 (Centre for Environmental Science and Engineering), IIT Kanpur, where they were further stored at -20˚C
160 in a deep freezer prior to analysis. For this study, the samples from the common period of offline and
161 online sampling (October-December 2019) from the two sites were analyzed for WSIS (SO$_4^{2-}$, NO$_3^-$, NH$_4^+$
162 and Cl$^-$) using an IC, and 32 metals (Al, Na, K, Ca, Ti, V, Cr, Mn, Fe, Ni, Cu, Zn, As, Se, Rb, Sr, Zr, Cd,
163 Sn, Sb, Ba, Pb, Cs, La, Ce, Pt, Tl, Mg, Li, Mo, Co and Pd) using an ICP-MS. More details of analytical
164 procedures are given in the instrumentation section.

165 **2.2.2 Online sampling**

166 At both IITD and IITMD site, high-resolution time-of-flight aerosol mass spectrometers (HR-ToF-AMS,
167 Aerodyne Research Inc., Billerica, MA) (Canagaratna et al., 2007; DeCarlo et al., 2006), equipped with
168 PM$_{2.5}$ aerodynamic lens (Peck et al., 2016) (Aerodyne Research Inc., Billerica, MA, USA) were installed
169 inside air-conditioned laboratories. Ambient fine particulate matters were sampled through PM$_{2.5}$ cyclone
170 (BGI, Mesa Labs. Inc.) inlet at IITD with a flow rate of 5 lpm (l/min) using a 2.44 m long stainless-steel
171 tubing (0.3 inch I.D and 0.4 inch O.D) and through black silicon tubing (0.19 inch I.D) at IITMD, placed
172 1.5 m above the rooftop. A Nafion dryer (MD-110-144P-4: Perma Pure, Halma, UK) was used to dry the
173 ambient aerosols to maintain the output RH at 20%. At IITD, data were collected from 12th October 2019-

174   31st December 2019 and 2nd June 2019-21st July 2019 during winter and summer campaigns respectively.

175   The data between 1st November and 14th November was not available, due to hardware issues in the AMS

176   during that period. At IITMD, data were only collected during winter campaign from 25th October 2019 to

177   31st December 2019.

178   Two Xact 625i ambient metal monitors (Cooper Environmental Services, Beaverton, Oregon, USA) were

179   installed inside temperature controlled laboratories at IITD and IITMD. Ambient aerosols were sampled

180   through a $PM_{2.5}$ inlet with a flow rate of 16.7 lpm. A separate sampling line of 2.44 meter (1.25 inch I.D)

181   for the Xact which was made of aluminium was installed. A heater was set up at the end of the sampling

182   line to ensure 45% RH set point. At IITD, sampling was carried out from 1st October 2019-31st December

183   2019 and 30th May 2019-25th July 2019 during the winter and summer campaign, respectively. However,

184   data between 16th July and 24th July were not available due to hardware breakdown. At IITMD, samples

185   were collected from 1st October 2019-31st December 2019 but data from 18th November to 26th

186   November 2019 and 30th November to 14th December 2019 were not available due to instrumental

187   problems.

188   Online measurements of inorganic ions (SO_4^{2-}, NO_3^-, NH_4^+ and Cl^-) from HR-ToF-AMS were compared

189   with the WSIS using an IC. Parallelly, heavy and trace metals obtained from Xact ambient metal mass

190   monitor were compared with the metal data from the offline filter measurements using an ICP-MS.

191   Though the sampling periods of AMS, Xact, and HVS were different for different seasons and different

192   sites as well (Table 1), only the common periods of online and offline sampling have been discussed in

193   this study for comparison.

194   Table 1. Sampling strategy and instrumentation used.

	Interval	IITD	IITMD
Quartz filter Sampling	3 days	January-May 2019	January-May 2019
		August-September 2019	August-September 2019
	24 hrs	June-July 2019	June-July 2019
		October-December 2019	October-December 2019
HR-Tof-AMS	2 mins	2nd June-21st July 2019	25th October-31st December 2019
		12nd October-31st December 2019	
Xact	30 mins	30th May-25th July 2019	1st October-31st December 2019
		1st October-31st December 2019	

195   Filters from the common periods were analysed for WSIS and heavy and trace metals using an IC and ICP-MS respectively.

2.3. Instrument details

2.3.1 WSIS measurements by IC and HR-ToF-AMS

For WSIS analysis, 9 sq.cm punch area of each collected filter was soaked in 30 ml of high purity milli-q water (resistivity-18.20 MΩ cm) for 12 hours in pre-cleaned borosilicate test tubes to ensure maximum solubility. The amount of water added, soaking time, etc. effect the solubility of the ions as well as the extent of extraction. Details can be found in our previous paper (Bhowmik et al., 2020). Soaked samples were filtered through 0.22 µm quartz filter papers to remove any suspended contaminations after an ultrasonication for 50 mins. Cl^-, NO_3^-, SO_4^{2-} and, NH_4^+ were measured for all the filter extracts by an IC (Metrohm 883 Basic IC plus for cations and 882 compact IC plus for anions). Separate columns for the analysis of cations and anions were installed in two separate modules. For anion and cation separation, an AS 5-250/4.0 chromatography column and C-6 column was used, respectively. The sample carried by 3.2 mM Na_2CO_3+1 mM $NaHCO_3$ solution and 2.7 mM HNO_3 solution in the anion and cation module separately passes through the charged columns to analyze each ion according to their polarity. The calibration was performed by a seven-point method with a range of standards prepared by the serial dilution from the stock solution standard of 10 ppm purchased from Metrohm. The uncertainty of the water-soluble inorganic ions measured by IC was estimated as 4% (coverage factor~2) by the approach described in Yardley et al. (2007).

HR-ToF-AMS measures size-resolved mass spectra of non-refractory particles (PM components that vaporize at 600°C and 10^{-5} Torr, e.g., organics, nitrate, sulphate, ammonium, and some chlorides) of submicron particulate matters. The details of this instrument can be found elsewhere (DeCarlo et al., 2006). Briefly, ambient aerosols are collected through an orifice of 100 μm diameter and focused into a narrow particle beam by an aerodynamic lens system installed inside the instrument, which has a transmission efficiency of > 50% for $PM_{2.5}$ (DeCarlo et al., 2006; Peck et al., 2016). The particle size is determined after analyzing the time of flight, i.e., time taken to travel along the length of the sizing chamber. The NR-PMs are then vaporized by hitting the vaporizer at 600°C and at a vacuum of 10^{-7} Torr. Further, the vaporized molecules are electronically ionized at 70 eV, followed by detection by a mass spectrometer as per their *m/z*. HR-ToF-AMS can be operated in W-mode or V-mode. For this study, it was operated in V-mode with a sampling time of 2 mins. Mass spectra (MS) mode, in which mass spectra of the components are measured, and particle time-of-flight (PToF) mode in which the size-resolved mass spectra are measured, are alternated in every 30s in 2 cycles. The HR-ToF-AMS was calibrated using standard protocols provided in our previous publication (Lalchandani et al., 2021; Singh et al., 2019).

227   To determine the mass concentration of NR-PMs, Unit mass resolution (UMR) analysis was done using

228   the SQUIRREL data analysis toolkit (version 1.59) programmed in IGOR Pro 6.37 software

229   (Wavemetrics, Inc., Portland, OR, USA). High resolution (HR) analysis was also done on the data set

230   using Peak Integrated Key Analysis (PIKA version 1.19) toolkit. A recommended collection efficiency

231   (CE) of 1 (Hu et al., 2017) was used for capture vaporizer. At the beginning and mid of each campaign at

232   the two sites, ionization efficiency (IE) calibration was performed by injecting mono-disperse 300 nm

233   ammonium nitrate and ammonium sulphate particles into AMS and a condensation particle counter

234   (Jayne et al., 2000). A relative ionization efficiency (RIE) of 4.05 and 4.35 was used for IITD and IITMD

235   site, respectively in case of NH_4. RIE of SO_4 was taken as 2.89 and 1.67 for IITD and IITMD,

236   respectively. For Org and Cl, by default a RIE of 1.4 and 1.3 were taken, respectively. More details can

237   be found in (Lalchandani et al., 2022).

2.3.2 Heavy and trace metal measurements by ICP-MS and Xact 625i

239   For the analysis of heavy and trace metals, 15 sq. cm area of each collected filter was digested in an acid

240   mix of 0.5 ml HF+1.5 ml HNO_3 for 4 hours within closed HDPE Teflon tubes using a Hot plate (Savillex-

241   HF resistive Model number 88888:00000). The temperature range should be ~90-120˚C to ensure

242   complete digestion of the elements. Further, 2.5 ml of $HClO_4$ was added to the precipitates, left over the

243   Teflon tube wall and the tubes were kept on the hot plate at 220-240˚C for another 4 hours with the lids

244   open for complete evaporation of the acid mix. Moreover, the residual was dissolved in 6N HNO_3 and

245   diluted with de-ionized water (resistivity-18.20 MΩ cm) followed by filtering through 0.22 μm quartz

246   filter papers prior analysis. Details can be found in our forthcoming paper. This method is well

247   established and used in many studies (Minguillón et al., 2012; Querol et al., 2008).

248   Thirty two metals (Al, Na, K, Ca, Ti, V, Cr, Mn, Fe, Ni, Cu, Zn, As, Se, Rb, Sr, Zr, Cd, Sn, Sb, Ba, Pb,

249   Cs, La, Ce, Pt, Tl, Mg, Li, Mo, Co and Pd) were analyzed for all filter extracts using an ICP-MS (Thermo

250   Scientific iCAP Q ICP-MS) at IIT Kanpur Environmental Engineering laboratory. Si could not be

251   determined in the filter samples because Si is the primary constituent of the quartz filters and hence

252   digested during sample preparation. Samples were first introduced to a nebulizer using an injector

253   attached to an autosampler for transformation into fine aerosol droplets followed by ionization at a very

254   high temperature (8000K) in Ar-plasma. The elements elute as per their *m/z*. A known concentration (5

255   ppb) of Ge was used as an internal standard to monitor the instrumental drift during the analysis. The

256   overall average drift was reported as ± 10%. The calibration was performed by ten-point method with a

257   range of mix standards prepared by the serial dilution from the High purity multi-element (35 elements)

258   standards (soluble in 1% HNO_3, 100 ppm) purchased from Sigma Aldrich.

259 The Xact 625i Ambient Metals Monitor (Cooper Environmental Services (CES), Beaverton, OR, USA)
260 uses X-ray fluorescence to measure the real-time elemental data in particulate matter. For this study, a
261 $PM_{2.5}$ inlet was used. Details of the instrument can be found in Furger et al., 2017. Briefly, aerosol
262 samples were collected on a Teflon filter tape followed by hitting the loaded area with X-rays and the
263 fluorescence measured by a silicon drift detector (SDD). Thirty elements: Al, Si, S, Cl, K, Ca, Ti, Cr, Mn,
264 Fe, Co, Ni, Cu, Zn, As, Se, Br, Rb, Sr, Zr, Mo, Cd, In, Sn, Sb, Te, Ba, Pb, Bi, and Bi were measured with
265 30 min time resolution. The Xact 625i was calibrated during each campaign using thin film standards for
266 the individual elements. The reproducibility was observed within ± 5%. Every midnight energy alignment
267 checks were performed for 15 mins (00:15 to 00:30) (for Cr, Pb, Cd and Nb). An uncertainty of ~10%
268 was reported by the manufacturer in an interference free situation (USEPA & Etv, 2012). This included
269 1.73% from flow (CEN, 2014), 5% for standard reproducibility or uncertainty during calibration
270 (USEPA, 1999) and 2.9% from term stability as reported in Tremper et al. (2018). More details on the
271 instrumental set up and stability check during the summer and winter campaign can be found in Rai et al.
272 (2020) and Shukla et al. (2021).

273 **3. Results and discussions**

274 **3.1. Online and offline measurements of WSIS and their comparison**

275 Large temporal variability was observed in both offline and online measurements of WSIS (NO_3^-, SO_4^{2-}
276 and, NH_4^+ and Cl^-) during the winter campaign and summer campaign at both sites. The inorganics data
277 with 2 mins interval from HR-ToF-AMS were averaged over the sampling period of the filters, i.e., 24
278 hours. The time series of NO_3^-, SO_4^{2-}, NH_4^+, and Cl^- during the summer and winter campaign at IITD and
279 winter campaign at IITMD are shown in Fig. SM1 in the supplementary material. Higher peaks of
280 inorganics were observed during 25th Oct-18th Nov during the winter campaign at IITD, which was the
281 agricultural crop-residue burning period (Nagar et al., 2017). During the winter campaign, NO_3^- was the
282 most abundant ion followed by SO_4^{2-}, NH_4^+ and Cl^- for both offline and online measurements at both the
283 sites whereas, during the summer campaign at IITD, NO_3^- was the most abundant ion followed by NH_4^+,
284 SO_4^{2-} and Cl^- in online measurement (HR-ToF-AMS). Similar results were observed in our companion
285 paper, Shukla et al. (2021). Interestingly, in the case of offline measurements during the summer
286 campaign at IITD, NO_3^- was least abundant, and the sequence changed as SO_4^{2-} > NH_4^+ > Cl^- > NO_3^-. The
287 average concentrations with their ranges are tabulated in Table SM1 in supplementary material, and the
288 mean, maximum and minimum concentration are shown in Fig. 2 using box plots.

Comparability and correlation between offline and online measurements were evaluated in this study by applying linear regression using offline data as the independent and online data as the dependent variable. The comparability of NH_4^+ measurements was observed to be good for both summer and winter campaigns at both sites. During the winter campaign, the correlations were $R^2=0.76$, and $R^2=0.89$, and the slopes were closer to 1 (0.99 for IITD and 0.93 for IITMD) for IITD and IITMD, respectively (Fig. 3). Interestingly during the summer campaign at IITD, though the correlation improves ($R^2=0.91$), the slope decreases to 0.49. This is likely because the vapor concentration of sulfuric acid (H_2SO_4) is higher during summers. As a result of which, the adsorption of sulfuric acid on PM deposited on the filter papers happens during summers which reacts with gaseous ammonia (NH_3) to form a relatively stable particulate $(NH_4)_2SO_4$ (Zhang et al., 2000), thus increasing ammonium concentration in the offline measurements during the warmer season, especially in the presence of dust (Nicolás et al., 2009).
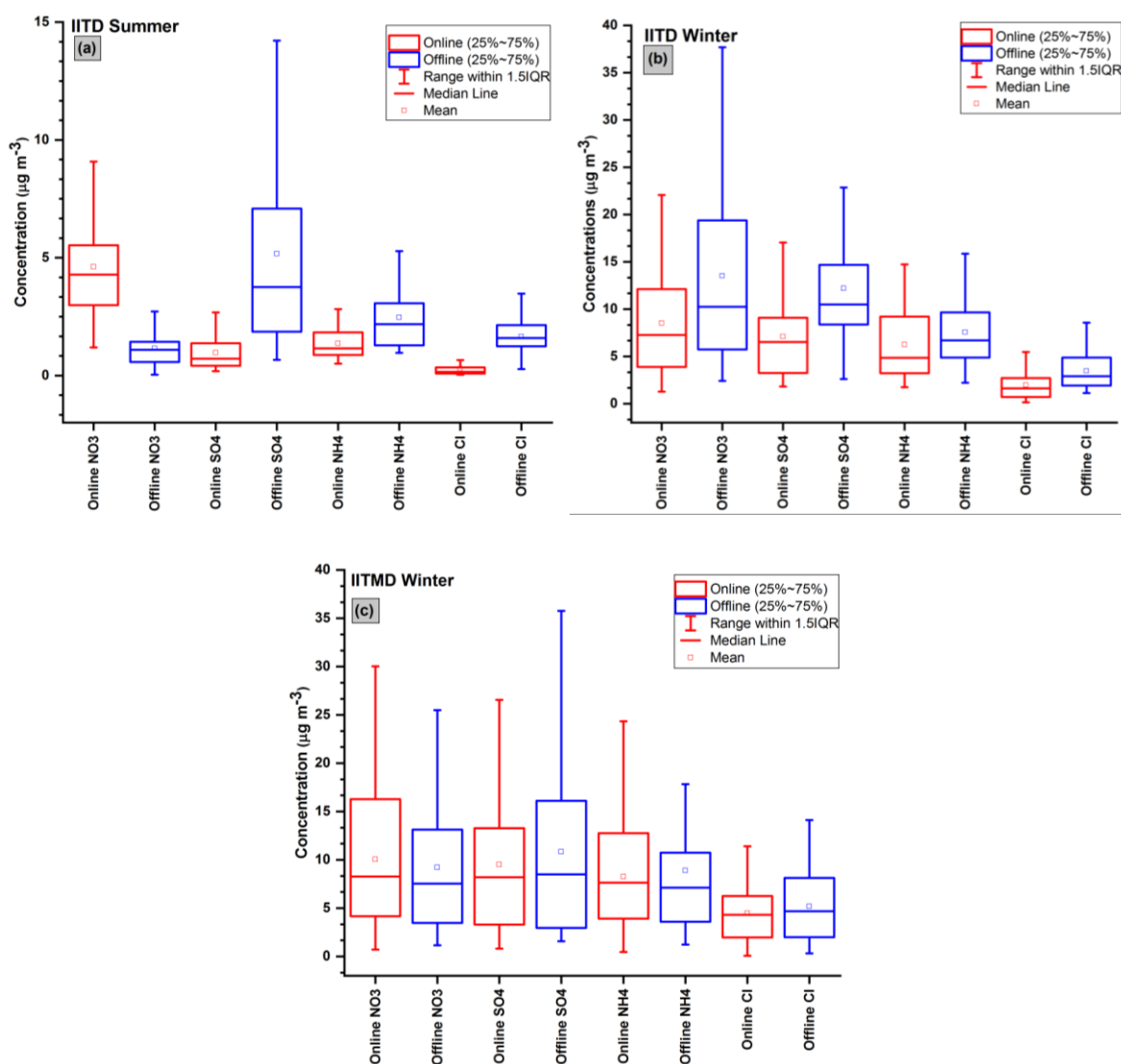
302 Fig.2. Box plots of online and offline measured secondary species (NO_3^-, SO_4^{2-} and, NH_4^+) and Cl^- during

303 (a) summer campaign at IITD, (b) winter campaign at IITD, and (c) winter campaign at IITMD site.

304 The filter-based measurements of SO_4^{2-} were higher than those from the online measurements for IITD

305 and IITMD during both the seasons (Fig. 2). Their comparability is characterized by a correlation

306 coefficient of R^2=0.93 with a slope of 0.17 and R^2=0.82 with a slope of 0.68 at IITD during the summer

307 and winter campaigns, respectively. Interestingly, offline SO_4^{2-} data correlates well with online SO_4^{2-} data

308 having a correlation coefficient of R^2=0.93 with a slope close to 1 (0.93) during the winter campaign at

309 IITMD (Fig. 3). A slope of less than 0.5 was observed in Malaguti et al., (2015) in Italy during the warm

310 period whereas the offline measurement of SO_4^{2-} was 34% lesser than the AMS measurements in Pandolfi

311 et al., (2014). The higher SO_4^{2-} concentrations on the un-denuded offline filter-based measurements could

312 be due to refractory sulfate (e.g., potassium or calcium sulfate). The higher filter-sulfate could also be

313 possibly because of the positive sampling artifact. The SO_2 is absorbed on the filter by the collected

314 alkaline particles (Nie et al., 2010). The higher concentration could also be due to the formation of

315 ammonium bi-sulfate or ammonium sulfate because of the reaction between gas-phase ammonia with the

316 acidic aerosols (Nicolás et al., 2009). Also, the un-denuded filter measurements could lead to higher

317 filter-sulfate. The interaction of gas phase ammonia with acidic aerosols can be minimized by using

318 denuders while collecting aerosols on the filters (Nault et al., 2020). Some studies suggested that the

319 organic sulfate, nitrate, and reduced nitrogen thermally decompose and/or under electron ionization in

320 AMS, producing inorganic ions. NO^+ and NO_2^+ contribute a significant fraction in organic nitrate (Day et

321 al., 2022) whereas, for organic sulfates, a large fraction of the signal is contributed by SO^+, SO_2^+, and

322 SO_3^+ (Chen et al., 2019). Though the additional inorganics are minimum, this could lead to possible

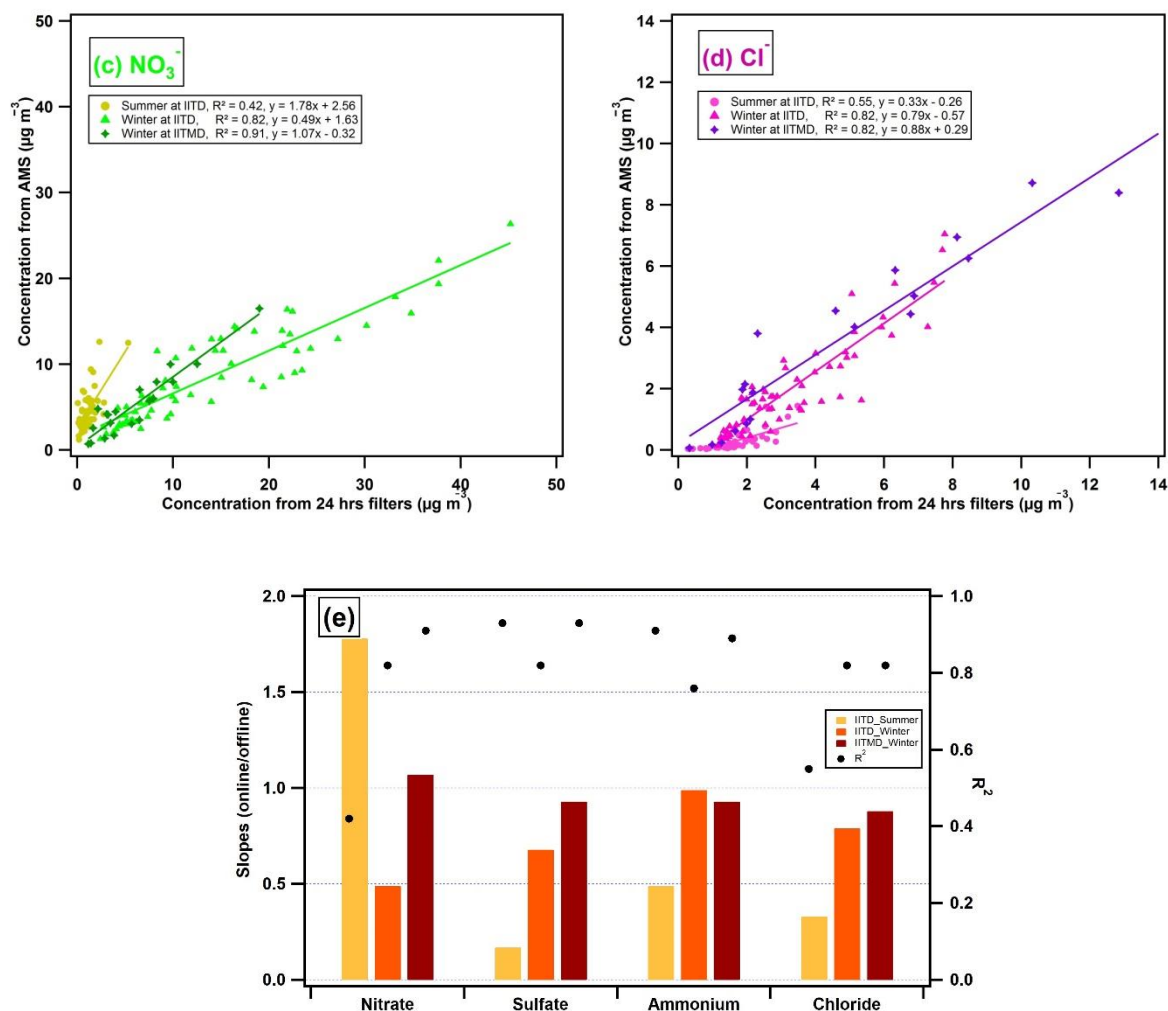323 marginal biases between the online and offline measurement of the inorganics.

324

325

326
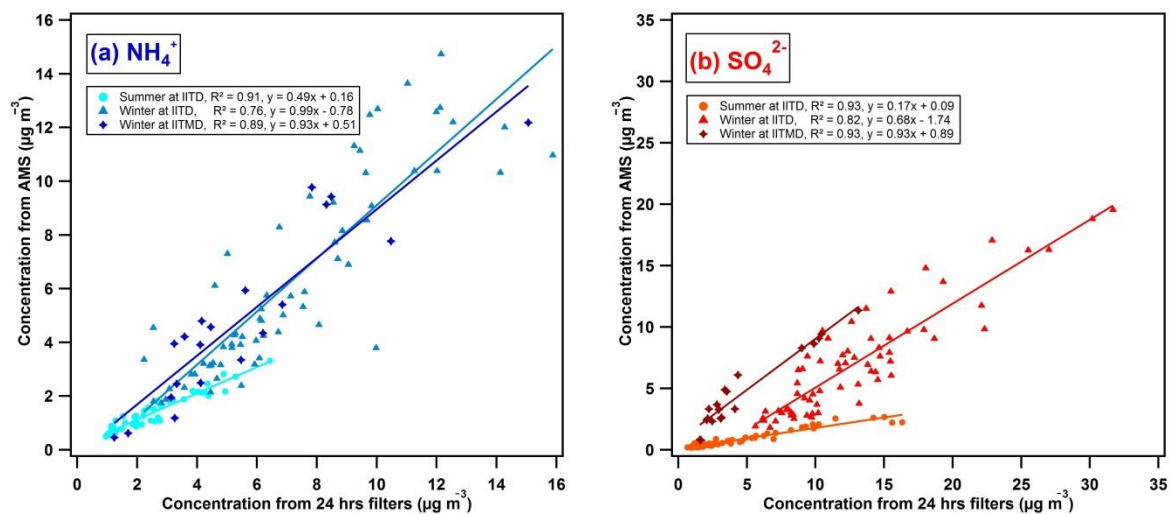
Fig.3. Scatter plots between online and offline measured (a) NH_4^+, (b) SO_4^{2-}, (c) NO_3^-, (d) Cl^- concentrations and (e) comparison of slopes (online/offline) and R^2 of the measured inorganic ions in $PM_{2.5}$ during summer and winter campaign at IITD and during winter campaign at IIITMD.

The online and offline NO_3^- measurements posed a good correlation during winter ($R^2 = 0.91$ and slope of 1.07 at IITMD, $R^2 = 0.82$ and slope of 0.49 at IITD) whereas the correlation worsens during summer at IITD ($R^2 = 0.42$ and slope of 1.78) (Fig. 3). The slopes and correlation coefficient for the WSIS are listed in Table 2. The NO_3^- concentrations measured by the HR-ToF-AMS were higher than the offline data during summer at IITD and during winter at IITMD whereas, filter-based measurements of NO_3^- were higher during winter at IITD (Fig. 2). The higher offline NO_3^- concentrations during winter at IITD can be possibly because of the positive artifact due to the absorption of gas-phase nitric acid (HNO_3) on the filter (Chow, 1995). Many studies (Chow et al., 2008; Kuokka et al., 2007; Malaguti et al., 2015) reported higher concentrations of NO_3^- from high time resolution measurements than filter-based measurements

13

due to the evaporation of ammonium nitrate collected on filters over the duration of sample collection (Pakkanen & Hillamo, 2002; Schaap et al., 2004; Kuokka et al., 2007). Pandolfi et al. (2014) observed NO_3^-_ HR-AMS/Filter ratios of ~1.7 at Barcelona and Montseny in Europe. This evaporation loss increases with the decrease of humidity and the increase of temperature (Chow et al., 2008; Takahama et al., 2004). Also, complete evaporation may occur beyond 25°C (Schaap et al., 2004). Chow et al. (2008) observed the evaporation loss from quartz filter to be more than 80% during the warm season in central California. The high temperature (35°C-48°C) during the long sampling hours (24 hours) may be a possible reason for the poor correlation between online and offline NO_3^- measurements during the summer campaign at IITD. Schaap et al. (2004) reported that the NO_3^- volatilization during a 24-h sampling period not only depends on the sampling instruments and ambient conditions, but also on sampling strategy. If the sampling strategy is evening-to-evening (24 hours), the samples will lose the night NO_3^- sampled during the night with the increasing temperature during the day. However, during morning-to-morning sampling strategy, the filters will collect the night NO_3^- quantitatively throughout the night, but the higher temperature in the afternoon of the previous day may promote the loss of afternoon NO_3^- from the filters (Malaguti et al., 2015). In this study, the sampling time was from 6:30 am to the next day 6.30 am. Therefore, the filter-based inorganic measurements suffered from a negative sampling artifact due to the evaporation of nitrate collected during the forenoon in a temperature of 20°C-25°C during the winter campaign and ~ 38°C-45°C during the summer campaign.

Table 2. Regression coefficients and slopes for the comparison of WSIS measured by HR-ToF-AMS and IC.

Sites	NO_3^-		SO_4^{2-}		NH_4^+		Cl^-	
	R^2	Slope	R^2	Slope	R^2	Slope	R^2	Slope
IITD Summer	0.42	1.78	0.93	0.17	0.91	0.49	0.55	0.33
IITD Winter	0.82	0.49	0.82	0.68	0.76	0.99	0.82	0.79
IITMD Winter	0.91	1.07	0.93	0.93	0.89	0.93	0.82	0.88

We observed higher Cl^- concentration in filter-based measurement than online measurement using HR-ToF-AMS during both campaigns at IITD and winter at IITMD. A good correlation of $R^2= 0.82$ with a slope of 0.79 and $R^2= 0.82$ with a slope of 0.88 was observed during the winter campaign at IITD and IITMD, respectively (Fig. 3). Interestingly, during the summer campaign at IITD the comparability was moderate with a correlation coefficient of $R^2= 0.55$ and a slope of 0.33. A correlation coefficient of $R^2= 0.83$ between Dp <10 μm measured with the MARGA and analyzed from Teflon filters was reported in Makkonen et al., (2012) during Feb-May. Lower temperature and higher RH during winter retains Cl^- in particulate phase for long enough to be detected which is not the case in summer. Further, Cl^- is

367 predominantly found in the coarse fraction. Also, while AMS only measures the NR-Cl⁻ (Manchanda et

368 al., 2021), e.g. NH_4Cl, which can vaporize at 600˚C but cannot measure Cl⁻ from refractory-KCl, IC

369 measures chloride from all the water-soluble chloride salts, including NH_4Cl and KCl. This probably

370 justifies the lower concentration of Cl⁻ in online measurement from AMS than filter-based measurements.

371 We also compared Cl⁻ measurements from Xact 625i with the measurements from IC. Interestingly, IC

372 measurements of Cl⁻ were found to be higher than Xact 625i measurements during summer at IITD and

373 winter at IITMD. The Cl measurements from Xact 625i were ~1.9 times higher than the measurements

374 from IC during winter at IITD (see fig. SM2 in supplementary material). The correlations were found to

375 be good during winter (R^2= 0.83 and 0.76 at IITD and IITMD respectively) and worsen during summer

376 (R^2= 0.27 at IITD), similar to what we observed for AMS_Cl⁻ and IC_Cl⁻. It could be due to the

377 differences in water-soluble fraction of chloride in the samples, as ionic concentration (IC) represents

378 water-soluble fraction whereas elemental concentration (Xact 625i) represents total concentration. Also, a

379 lot particulate bound chloride in the atmosphere is in the form of ammonium chloride (Manchanda et al.,

380 2021). Part of the ammonium chloride collected during the day long offline sampling would have

381 vaporized, giving lower concentration from IC measurements. Further investigation is needed to draw a

382 firm conclusion.

3.2 Online and offline measurements of heavy and trace metals and their comparison

384 For the inter-comparison of heavy and trace metal concentrations from Xact 625i and ICP-MS, the half-

385 hourly Xact 625i data were averaged to 24 hours filter sampling interval. A total of 32 elements were

386 analyzed on each filter using ICP-MS while, 27 elements were measured in Xact 625i at IITD during

387 summer and winter campaign, and 30 elements were measured in Xact 625i at IITMD during the winter

388 campaign. The spatial and temporal variations of the crustal and trace elements are shown in Fig. SM3. Al

389 and Ca concentrations were the most abundant in ICP-MS and Xact measurements respectively during the

390 summer season (Fig. 4a, 5a & 5b) because of the increase in the crustal activities whereas K

391 concentrations were significantly high for both the measurements during winter (Fig. 4d, 4g, 5c, 5d, 5e

392 and 5f) due to mass-scale agricultural crop-residue burning in the adjoining states of Punjab and Haryana.

393 Elements emitted from anthropogenic activities, e.g., coal-fired power plants (As, Se, Hg, Pb), traffic

394 emissions (Cr, Pb, Mn), wear debris emission (Cu, Cd, Fe, Ga, Mn, Mo), etc. are found to be in higher

395 concentration during winter campaign than summer campaign for both the measurements. Similar results

396 were observed in our companion paper Shukla et al. (2021). The average values of metals along with their

397 ranges are tabulated in Table SM2 and the statistics involved mean, upper, and lower values of some

398 major elements are shown in Fig. 4. Box plots for rest of the metals can be found in Fig. SM4.

399

400
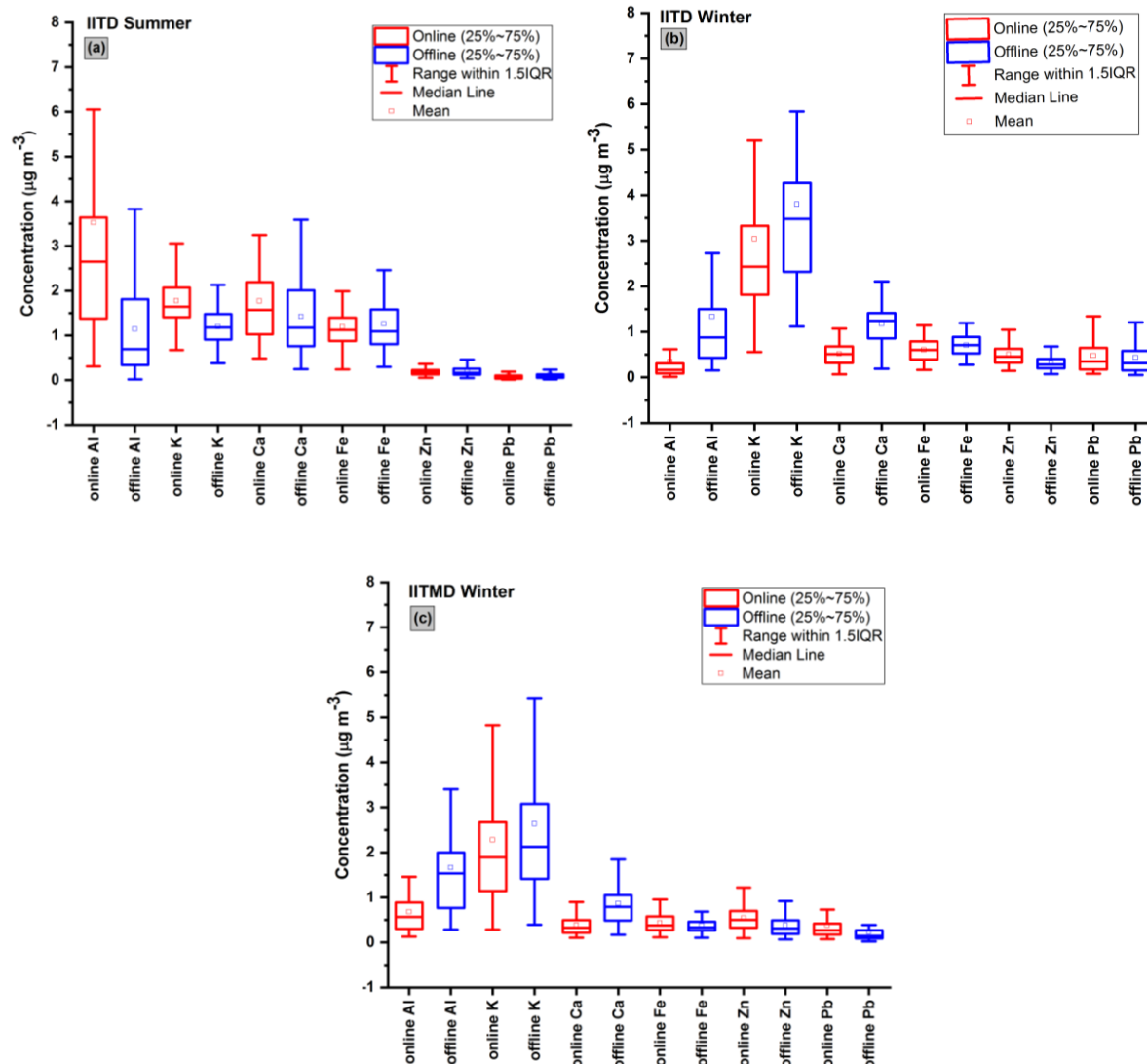
Fig.4. Box plots of some major elements measured offline and online during (a) summer campaign at IITD, (b) winter campaign at IITD, and (c) winter campaign at IITMD site. The box plots for rest of the heavy and trace elements are shown in fig. SM4 of the supplementary material.

The trends of the elemental concentration in decreasing order for both ICP-MS and Xact measurements during summer and winter at IITD and winter at IITMD are shown in Fig. SM5. The trace metals such as Cd, Mn, Mo, Ba, Pd etc. contribute a small portion in $PM_{2.5}$ in terms of their mass concentration but have a significant effect on human health. Fractions of elements in total element concentration for both the measurements during summer and winter campaign at IITD and during winter campaign at IITMD were shown in Fig. 5.

(a) IITD Summer Xact measurements

Al	39.53%
K	19.91%
Ca	19.84%
Fe	13.41%
Others	7.30%

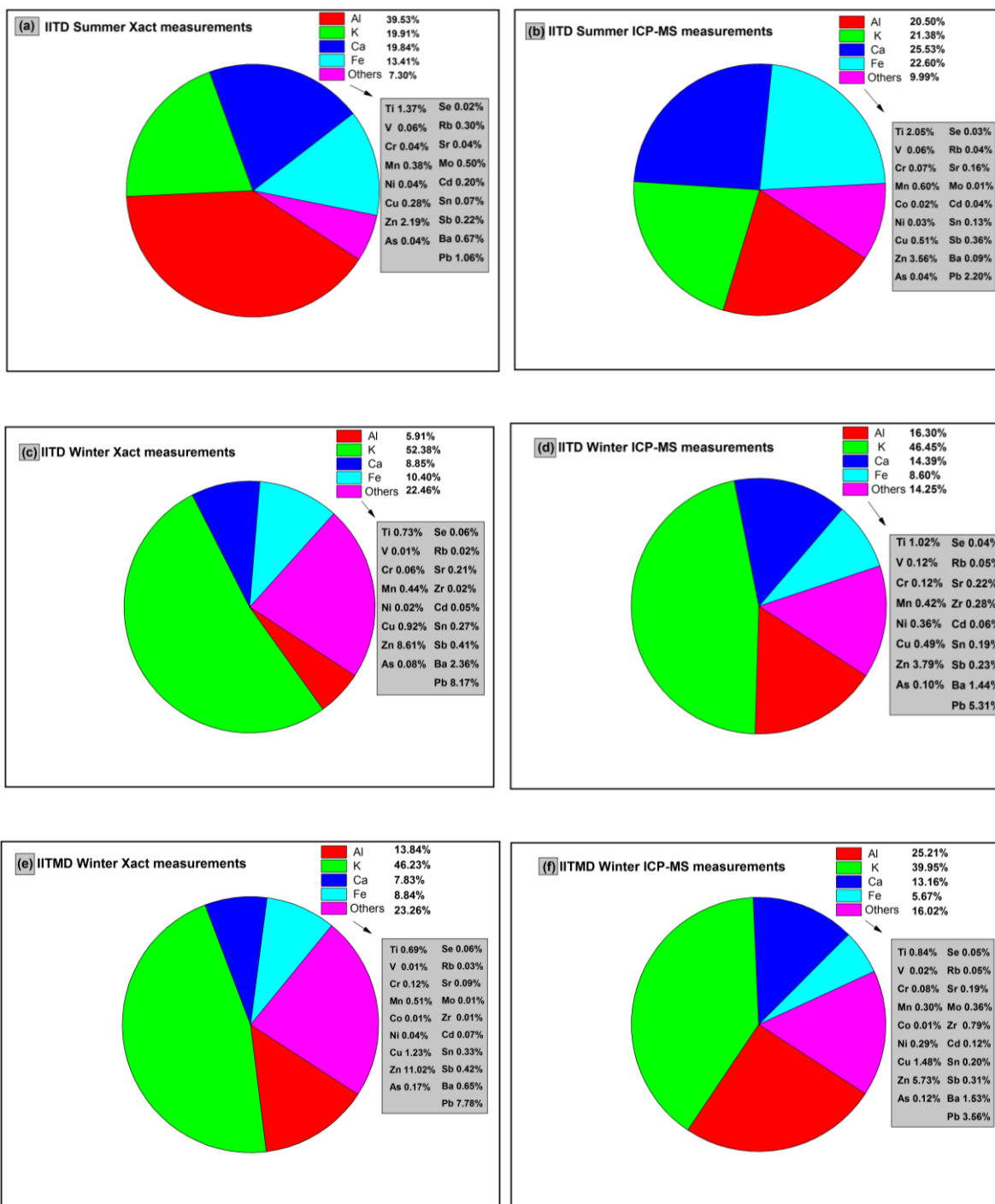|	
Ti 1.37%	Se 0.02%
V 0.06%	Rb 0.30%
Cr 0.04%	Sr 0.04%
Mn 0.38%	Mo 0.50%
Ni 0.04%	Cd 0.20%
Cu 0.28%	Sn 0.07%
Zn 2.19%	Sb 0.22%
As 0.04%	Ba 0.67%
	Pb 1.06%

(b) IITD Summer ICP-MS measurements

Al	20.50%
K	21.38%
Ca	25.53%
Fe	22.60%
Others	9.99%

Ti 2.05%	Se 0.03%
V 0.06%	Rb 0.04%
Cr 0.07%	Sr 0.16%
Mn 0.60%	Mo 0.01%
Co 0.02%	Cd 0.04%
Ni 0.03%	Sn 0.13%
Cu 0.51%	Sb 0.36%
Zn 3.56%	Ba 0.09%
As 0.04%	Pb 2.20%

410

(c) IITD Winter Xact measurements

Al	5.91%
K	52.38%
Ca	8.85%
Fe	10.40%
Others	22.46%

Ti 0.73%	Se 0.06%
V 0.01%	Rb 0.02%
Cr 0.06%	Sr 0.21%
Mn 0.44%	Zr 0.02%
Ni 0.02%	Cd 0.05%
Cu 0.92%	Sn 0.27%
Zn 8.61%	Sb 0.41%
As 0.08%	Ba 2.36%
	Pb 8.17%

(d) IITD Winter ICP-MS measurements

Al	16.30%
K	46.45%
Ca	14.39%
Fe	8.60%
Others	14.25%

Ti 1.02%	Se 0.04%
V 0.12%	Rb 0.05%
Cr 0.12%	Sr 0.22%
Mn 0.42%	Zr 0.28%
Ni 0.36%	Cd 0.06%
Cu 0.49%	Sn 0.19%
Zn 3.79%	Sb 0.23%
As 0.10%	Ba 1.44%
	Pb 5.31%

411

(e) IITMD Winter Xact measurements

Al	13.84%
K	46.23%
Ca	7.83%
Fe	8.84%
Others	23.26%

Ti 0.69%	Se 0.06%
V 0.01%	Rb 0.03%
Cr 0.12%	Sr 0.09%
Mn 0.51%	Mo 0.01%
Co 0.01%	Zr 0.01%
Ni 0.04%	Cd 0.07%
Cu 1.23%	Sn 0.33%
Zn 11.02%	Sb 0.42%
As 0.17%	Ba 0.65%
	Pb 7.78%

(f) IITMD Winter ICP-MS measurements

Al	25.21%
K	39.95%
Ca	13.16%
Fe	5.67%
Others	16.02%

Ti 0.84%	Se 0.05%
V 0.02%	Rb 0.05%
Cr 0.08%	Sr 0.19%
Mn 0.30%	Mo 0.36%
Co 0.01%	Zr 0.79%
Ni 0.29%	Cd 0.12%
Cu 1.48%	Sn 0.20%
Zn 5.73%	Sb 0.31%
As 0.12%	Ba 1.53%
	Pb 3.56%

412

413 Fig.5. Fractions (%) of elements in total element concentration in $PM_{2.5}$ presented in pie format for online

414 (a,c,e) and offline (b,d,f) measurements during winter and summer at IITD and during winter at IITMD.

415 MDLs for ICP-MS measurements were calculated according to Escrig Vidal et al., (2009), and MDLs for

416 Xact 625i were obtained from the manufacturer. MDLs for the Xact 625i and ICP-MS are listed in Table

SM2 in the supplementary material. Though the half-hourly Xact data were averaged to 24 hours to the corresponding interval of the filter sampling, for comparability check, MDLs of Xact 625i measurements were taken for 30 mins sampling time while MDLs of filter-based elemental measurements were calculated for 24 hours. Elements having data below $3 \times$ MDL were discarded from further examination and unreliable as values below $3 \times$ MDL would lead to higher uncertainty (Furger et al., 2017). The elements K, Ca, Ti, Mn, Fe, Ba, and Pb have >80% of their values above both offline and online MDLs, and thus the data quality is reliable. Further, Ni, Mo, Zr have higher blank concentrations, and thus the data is not reliable for ICP-MS measurements. The comparability of the elements measured online using Xact 625i with those analysed using an ICP-MS, was checked for the common elements in these two measurements (21 elements for IITD and 23 elements for IITMD) and is shown in Fig. 6.
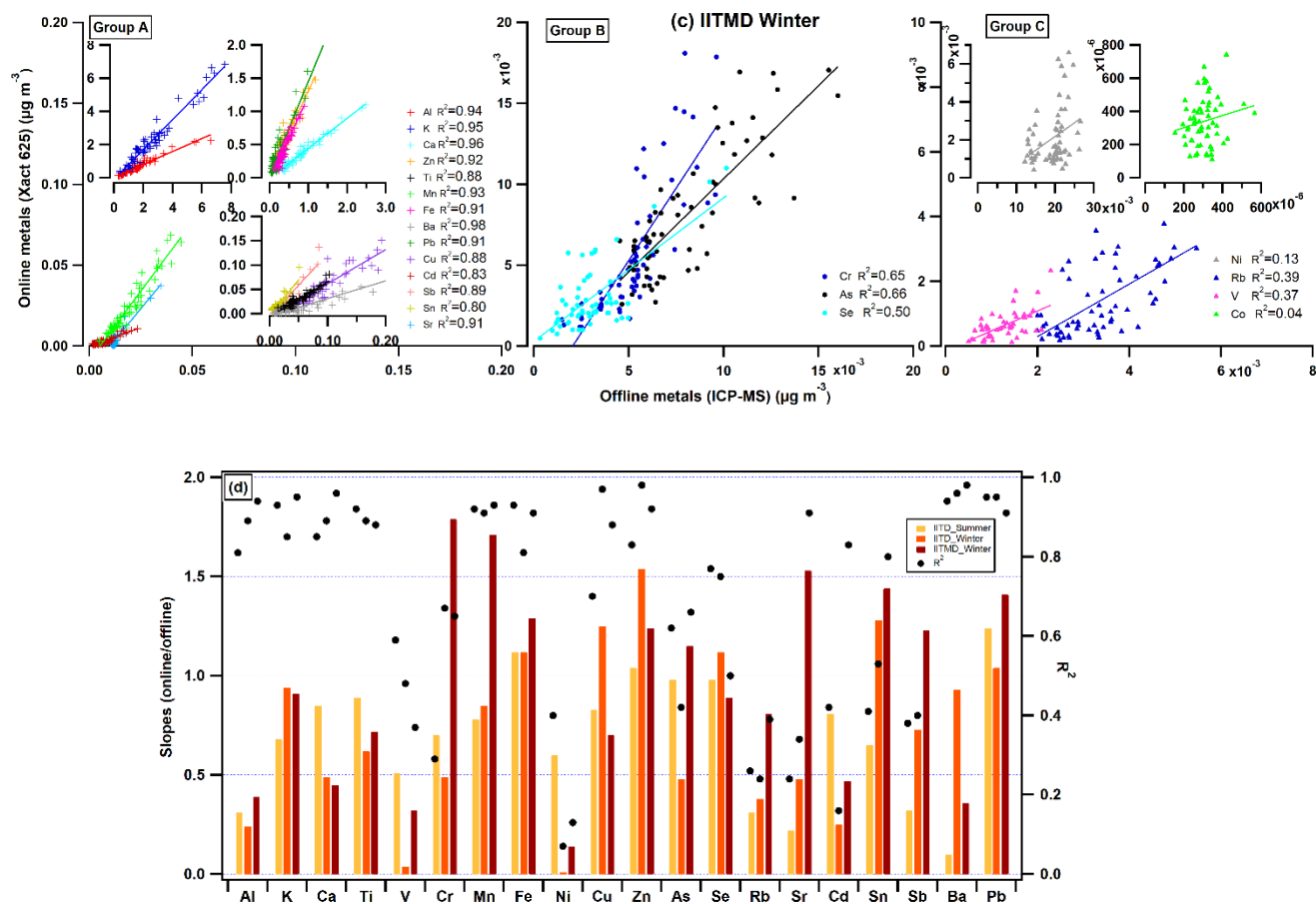
429

430
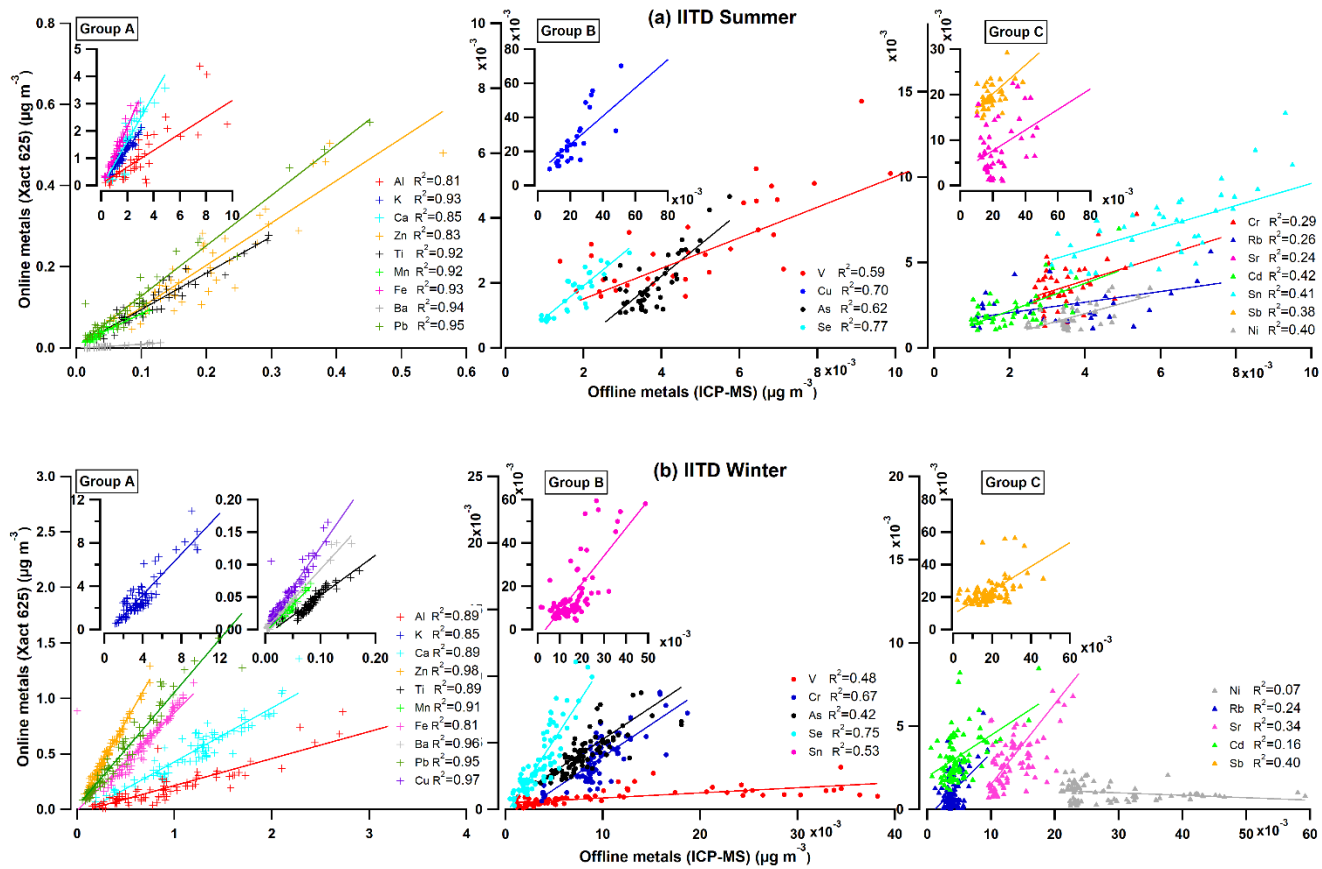
Fig. 6. Scatter plots and regression lines of Xact 625i vs. ICP-MS data for groups A, B, and C during (a) summer at IITD, (b) winter at IITD, (c) winter at IITMD, and (d) comparison of slopes (online/offline) & R^2 of the measured heavy and trace metals in $PM_{2.5}$ during the summer and winter campaign at IITD and winter campaign at IIITMD.

Based on their comparability characteristics, elements were grouped under 3 categories. Group A showed excellent linearity between the two methods with a correlation coefficient of $R^2 > 0.8$. Overall, group A consists of Al, K, Ca, Ti, Mn, Fe, Cu, Zn, Ba, and Pb during winter at IITD whereas, Cu showed in another group during summer at IITD. Though Sr, Cd, Sn, Sb had average values below MDLs and posed a lower correlation coefficient at IITD, interestingly, Sr, Cd, Sn, and Sb joined group A during winter at IITMD. To distinguish the potential difference in accuracy between the two methods, intercepts were not forced to be zero. The slopes are important, which indicate biases between the two measurements. The slopes of Zn, Fe, and Pb were closer to unity during summer at IITD (Fig. 6). K, Fe, Cu, Zn, Ba, and Pb achieved a slope of 0.94-1.25 during winter at IITD whereas, Mn, Fe, Zn, Pb, Sr, Sn, and Sb pose a slope slightly higher than unity during winter at IITMD (Fig. 6). A slight difference in cut-off value for the

445 particle size can reduce the slopes from unity and produce ~10% difference in collected mass (Panteliadis
446 et al., 2012). The slopes and the correlation coefficients are listed in Table 3.

447 In a comparison study conducted by USEPA & Etv. (2012) between Xact 625i and ICP-MS
448 measurements, Ca, Cu, Mn, Pb, Se, and Zn were highly correlated except Cu. Cu was close to the MDL
449 values of ICP-MS and Xact 625i. A good agreement was observed between Xact 625i and offline
450 measurements using ED-XRF in South Korea by Park et al., (2014). The comparability between Xact
451 measurements and ICP-MS measurements was checked for the elements As, Ba, Ca, Cr, Cu, Fe, K, Mn,
452 Ni, Pb, Se, Sr, Ti, V, and Zn in Tremper et al. (2018). They observed an average R^2 of 0.93 and a slope of
453 1.07 for these elements. In the study by Furger et al., (2017) during a warmer season in Switzerland, an
454 excellent correlation ($R^2>0.95$) was found for Xact and ICP-OES/MS measurements of S, K, Ca, Ti, Mn,
455 Fe, Cu, Zn, Ba, and Pb. However, they found that the elemental measurements by Xact 625i were 28%
456 higher than ICP-OES/MS measurements for these 10 elements. In our study, Xact measurements of Fe,
457 Cu, Zn, and Pb yielded an average of 24% higher mass concentrations than ICP-MS measurements for
458 Group A elements during winter at IITD. Xact measurements were systematically 10% (average) higher
459 than ICP for Zn, Fe, and Pb during summer at IITD, whereas; we obtained an average of 41% higher
460 Xact measurements than ICP for Mn, Fe, Zn, Pb, Sr, Sn, and Sb during winter at IITMD in Group A
461 elements.

462 Group B was characterized by moderate linearity having $R^2\sim0.4$-0.8 and consisted of the elements V, Cu,
463 As, and Se during summer at IITD; V, Cr, As, Se, Sn during winter at IITD and Cr, As and Se during
464 winter at IITMD. These elements in Group B had their values very close to or below MDLs of at least
465 one of the analysis methods. During winter at both sites, Cr and As from ICP-MS have ~50-65% of their
466 values below MDLs, whereas ~68-72% of their values were above the MDLs of Xact 625i. Though some
467 of the elements in this group in different seasons have slopes near or greater than unity (see Table 3) like
468 Group A, their comparison is not statistically feasible.

469 Table 3. Regression coefficients and slopes for the comparison of Xact 625i and ICP-MS measurements.

Sites	Group A	Slope	R^2	Group B	Slope	R^2	Group C	Slope	R^2
	Al	0.31	0.81	V	0.51	0.59	Cr	0.7	0.29
	K	0.68	0.93	Cu	0.83	0.70	Co	-	-
	Ca	0.85	0.85	As	0.98	0.62	Rb	0.31	0.26
IITD Summer	Zn	1.04	0.83	Se	0.98	0.77	Sr	0.22	0.24
	Ba	0.1	0.94				Mo	-	-

	Element			Element			Element		
	Ti	0.89	0.92				Cd	0.81	0.42
	Mn	0.78	0.92				Sn	0.65	0.41
	Fe	1.12	0.93				Sb	0.32	0.38
	Pb	1.24	0.95				Ni	0.6	0.4
IITD Winter	Al	0.24	0.89	V	0.04	0.48	Ni	0.01	0.07
	K	0.94	0.85	Cr	0.49	0.67	Rb	0.38	0.24
	Ca	0.49	0.89	As	0.48	0.42	Sr	0.48	0.34
	Ti	0.62	0.89	Se	1.12	0.75	Zr	-	-
	Mn	0.85	0.91	Sn	1.28	0.53	Cd	0.25	0.16
	Fe	1.12	0.81				Sb	0.73	0.40
	Cu	1.25	0.97						
	Zn	1.54	0.98						
	Ba	0.93	0.96						
	Pb	1.04	0.95						
IITMD Winter	Al	0.39	0.94	Cr	1.79	0.65	Ni	0.14	0.13
	K	0.91	0.95	As	1.15	0.66	Rb	0.81	0.39
	Ca	0.45	0.96	Se	0.89	0.5	Mo	-	-
	Ti	0.72	0.88				Zr	-	-
	Mn	1.71	0.93				V	0.32	0.37
	Fe	1.29	0.91				Co	0.36	0.04
	Cu	0.70	0.88						
	Zn	1.24	0.92						
	Ba	0.36	0.98						
	Pb	1.41	0.91						
	Sr	1.53	0.91						
	Cd	0.47	0.83						
	Sn	1.44	0.8						
	Sb	1.23	0.89						

470   The Group C elements, e.g., Ni, Rb, Sr, Zr, Cd, and Sb during summer at IITD; Cr, Co, Rb, Sr, Mo, Cd,

471   Sn, Sb, and Ni during winter at IITD and, Ni, Rb, Mo, Zr, V, and Co during winter at IITMD are

472   characterized by their bad correlation ($R^2 < 0.4$). Interestingly, measurements of some element e.g. Mo

473   during summer and winter at IITD and IITMD respectively, Co during summer at IITD, and Zr during

474   winter at both sites from both the methods did not correlate at all. For most of the elements in this group,

475   70-85% of measurements were below both method's MDLs and rest of the data were below $3 \times$ MDLs.

476   The high and variable blank concentrations of these elements increased the MDL values in ICP-MS

477   measurement. The particle size dependent self-absorption effect and line interference between different

478   elements in Xact measurement could also increase the MDL values (Furger et al., 2017). This is probably

479   the reason for the values lower than MDLs for the elements in this group.

480   Overall, we observed 10-40% higher Xact measurements than ICP for some of the elements in Group A

481   during different seasons. The difference in the Xact and High-volume sampler inlet location and their

482   distance from the road can cause such difference in measurements (Furger et al., 2017). In the case of dust

483   resuspension from vehicular traffic, the number concentration of finer particulate matter tends to decrease

484   sharply within an increment of just 50m from the roadway (Hagler et al., 2009). In this study, we tried to

485   co-locate the two sample inlets, but it could not be avoided. Also, IITD and IITMD are both very close

486   (<200 m) to a roadway with moderate to heavy-duty traffic. The differences in online and offline

487   measurements may indicate a gradient in some elements due to very close proximity to heavy-duty traffic.

488   Also, the different temperatures of the sample inlets may give rise to a difference in measured

489   concentrations from both methods (Tremper et al., 2018). In this study, the blank corrected ICP-MS

490   measurements may result in overestimation or underestimation due to variable and high blank

491   concentration. The difference can also occur due to the digestion recovery rate for the digestion protocol

492   used for the filter analysis. Moreover, if the ambient elemental concentration is much lower than the

493   standards used for calibration of Xact, such differences may occur (Indresand et al., 2013).

494   **4. Conclusion**

495   Atmospheric WSIS (NO_3^-, SO_4^{2-}, NH_4^+, Cl^-) and heavy and trace elements in $PM_{2.5}$ were measured using

496   offline methods (IC for WSIS and ICP-MS for elements) and online methods (HR-ToF-AMS for

497   inorganics and Xact 625i for elements). These measurements were compared to assess the measurement

498   quality and sampling artifacts of these measurement techniques in the heavily polluted Delhi-NCR for

499   two different metrological conditions (winter and summer season). Field campaigns were conducted at

500   two NCR sites, namely, IITD during June-July 2019 and Oct-Dec 2019 and at IITMD during Oct-Dec

501   2019. The key findings of this study are summarized below.

502   • NH_4^+ concentrations from the IC and HR-ToF-AMS, compared well during winter with a slope

503   of 0.99 at IITD and 0.93 at IITMD. Interestingly, NH_4^+ concentrations were higher in offline

504   measurements during summer at IITD. The decrease in slope was probably due to the formation

505   of particulate $(NH_4)_2SO_4$.

506   • Offline SO_4^{2-} measurements were higher (with a slope of 0.17 during summer at IITD and 0.8

507   and 0.93 during winter at IITD and IITMD, respectively) during both seasons at both the sites

508   due to the positive sampling artifact. The absorption of SO_2 and the oxidation or condensation

509   process may result in additional sulphate.

510   • Lower NO_3^- concentrations (with a slope of 1.78 during summer at IITD and 1.07 during winter

511   at IITMD) were observed in the offline measurement during summer at IITD and during winter

512   at IITMD because of the evaporation of NH_4NO_3 from the filter substrates.   The evaporative

513   loss of nitrate from the filters was minimal in winter at IITMD. It aggravated during summer at

514   IITD due to the evaporation of ammonium nitrate in such a high temperature (35˚C-48˚C) range.

515   The higher NO_3^- concentrations (slope~0.49) in the filters than HR-ToF-AMS measurements

516   during winter at IITD can be due to the absorption of gas-phase HNO_3 on the filter.

517   • Offline Cl^- was consistently higher (with a slope of 0.33 during summer at IITD and 0.79 and

518   0.88 during winter at IITD and IITMD, respectively) than HR-ToF-AMS measurements during

519   both seasons at both sites mainly because HR-ToF-AMS only measures the $NR-Cl^-$ whereas, the

520   offline Cl^- measurements includes chloride from all the water-soluble chloride salts. The

521   comparability degrades during summer due to the volatile nature of Cl^- in higher temperatures

522   and lower RH.

523   • The elements were grouped into three categories (Group A, B and C) according to their

524   comparability characteristics. The elemental data from Xact 625i were highly correlated

525   (R^2>0.8) with ICP-MS measurements of the 24 hr filters for Group A elements (Al, K, Ca, Ti,

526   Zn, Mn, Fe, Ba, and Pb). The Cu also showed up in this group during winter at IITD. About

527   80% of the data for these elements were above MDLs for both the methods. Though Sn, Sb, and

528   Cd had values below MDLs of one or both the methods, interestingly, they were highly

529   correlated (R^2>0.8) and, slopes are very close to unity for Sn and Sb during winter at IITMD.

530   The correlation coefficients > 0.8 for the elements in Group A indicated the high precision of

531   the online and offline measurements. Hence, these elements from any of these methods can be

532   reliably used for modelling studies.

533   • The elements under Group B had their values closer to or below at least one of the method's

534   MDLs. Cr and As had ~50-65% of their values below ICP-MS MDLs from ICP-MS, whereas

535   ~68-72% of their values were above Xact 625i MDLs during winter at both sites.

- Elements like Ni, Mo, and Zr measured from ICP-MS were not reliable due to their higher and variable blank concentrations. No conclusion on their measurement accuracy by the two methods can be drawn.
- In summary, the daily averaged half-hourly Xact 625i measurements were 10-40% higher than 24 hr filter measurements by ICP-MS depending upon the seasons, sites and elements in Group A. Distance between two inlets for the two methods, distance of the inlets from the roadway, line interference between two elements in Xact measurements, particle size, sampling strategy, filter type, higher and variable concentrations in blank filters and digestion protocol for ICP measurements can cause the difference in measurements between the two methods.

The above findings highlight the measurement methods' accuracy and implement the particular type of measurements as needed. Denuders could be effective in avoiding the overestimation problems of ammonium and sulphate in filter measurements and improve the comparison. Also, teflon filters instead of quartz filters in the un-denuded sampler are reported to give better comparison for sulphate. The MDLs in the Xact 625 measurements are higher than the MDLs for the offline method. Depending on the objective of the campaign, Xact 625 can be deployed for a longer time interval to analyse the elements that are below their MDLs. The high resolution real-time monitoring of non-refractory organics, inorganics by HR-ToF-AMS and elements by Xact comes at the cost of high sensitivity in MDLs, calibrations and cost. Whereas, cost effectiveness of conventional samplers makes it practical to deploy in larger numbers at multi-sites simultaneously. Overall, high resolution real time sampling provides a rich dataset for high and small pollution episodes. Future work should involve using different filter substrates and different digestion protocols to re-evaluate the difference between these online and offline methods. Although this study compares the PM species, a comparison of full source apportionment analysis between online and offline methods should be done for more qualitative and quantitative insights.

Author contribution

HSB performed the offline analysis, data processing and wrote the manuscript. JD collected the AMS data at IITD. AS and VL carried out the Xact and AMS data collection and processing respectively. NR, MK, VS and SNT were involved with the supervision and conceptualization. All co-authors contributed to the paper discussion and revision.

Declaration of interests

The authors declare that they have no conflict of interest.

574 **Reference**

575 Bhowmik, H. S., Naresh, S., Bhattu, D., Rastogi, N., Prévôt, A. S. H., & Tripathi, S. N. (2020). Temporal and spatial

576   variability of carbonaceous species (EC; OC; WSOC and SOA) in PM2.5 aerosol over five sites of Indo-

577   Gangetic Plain. *Atmospheric Pollution Research*, *12*(June 2020), 375–390.

578   https://doi.org/10.1016/j.apr.2020.09.019

579 Chen, Y., Xu, L., Humphry, T., Hettiyadura, A. P. S., Ovadnevaite, J., Huang, S., Poulain, L., Schroder, J. C.,

580   Campuzano-Jost, P., Jimenez, J. L., Herrmann, H., O'Dowd, C., Stone, E. A., & Ng, N. L. (2019). Response

581   of the Aerodyne Aerosol Mass Spectrometer to Inorganic Sulfates and Organosulfur Compounds:

582   Applications in Field and Laboratory Measurements. *Environmental Science and Technology*, *53*(9), 5176–

583   5186. https://doi.org/10.1021/acs.est.9b00884

584 Chow, J. C. (1995). Measurement methods to determine compliance with ambient air quality standards for

585   suspended particles. *Journal of the Air and Waste Management Association*, *45*(5), 320–382.

586   https://doi.org/10.1080/10473289.1995.10467369

587 Chow, J. C., Watson, J. G., Lowenthal, D. H., Park, K., Doraiswamy, P., Bowers, K., & Bode, R. (2008).

588   Continuous and filter-based measurements of PM2.5 nitrate and sulfate at the Fresno Supersite. *Environmental*

589   *Monitoring and Assessment*, *144*(1–3), 179–189. https://doi.org/10.1007/s10661-007-9987-5

590 Day, D., Campuzano-Jost, P., Nault, B., Palm, B., Hu, W., Guo, H., Wooldridge, P., Cohen, R., Docherty, K.,

591   Huffman, J. A., de Sá, S., Martin, S., & Jimenez, J. (2021). A Systematic Re-evaluation of Methods for

592   Quantification of Bulk Particle-phase Organic Nitrates Using Real-time Aerosol Mass Spectrometry.

593   *Atmospheric Measurement Techniques Discussions*, *2*(3), 1–35. https://doi.org/10.5194/amt-2021-263

594 DeCarlo, P. F., Kimmel, J. R., Trimborn, A., Northway, M. J., Jayne, J. T., Aiken, A. C., Gonin, M., Fuhrer, K.,

595   Horvath, T., Docherty, K. S., Worsnop, D. R., & Jimenez, J. L. (2006). Field-deployable, high-resolution,

596   time-of-flight aerosol mass spectrometer. *Analytical Chemistry*, *78*(24), 8281–8289.

597   https://doi.org/10.1021/ac061249n

598   Escrig Vidal, A., Monfort, E., Celades, I., Querol, X., Amato, F., Minguillón, M. C., & Hopke, P. K. (2009).
599   Application of optimally scaled target factor analysis for assessing source contribution of ambient PM10.
600   *Journal of the Air and Waste Management Association*, *59*(11), 1296–1307. https://doi.org/10.3155/1047-
601   3289.59.11.1296

602   Furger, M., Minguillón, M. C., Yadav, V., Slowik, J. G., Hüglin, C., Fröhlich, R., Petterson, K., Baltensperger, U.,
603   & Prévôt, A. S. H. (2017). Elemental composition of ambient aerosols measured with high temporal resolution
604   using an online XRF spectrometer. *Atmospheric Measurement Techniques*, *10*(6), 2061–2076.
605   https://doi.org/10.5194/amt-10-2061-2017

606   Gani, S., Bhandari, S., Seraj, S., Wang, D. S., Patel, K., Soni, P., Arub, Z., Habib, G., Hildebrandt Ruiz, L., & Apte,
607   J. S. (2019). Submicron aerosol composition in the world's most polluted megacity: The Delhi Aerosol
608   Supersite study. *Atmospheric Chemistry and Physics*, *19*(10), 6843–6859. https://doi.org/10.5194/acp-19-
609   6843-2019

610   Hagler, G. S. W., Baldauf, R. W., Thoma, E. D., Long, T. R., Snow, R. F., Kinsey, J. S., Oudejans, L., & Gullett, B.
611   K. (2009). Ultrafine particles near a major roadway in Raleigh, North Carolina: Downwind attenuation and
612   correlation with traffic-related pollutants. *Atmospheric Environment*, *43*(6), 1229–1234.
613   https://doi.org/10.1016/j.atmosenv.2008.11.024

614   Hong, C., Zhang, Q., Zhang, Y., Davis, S. J., Tong, D., Zheng, Y., Liu, Z., Guan, D., He, K., & Schellnhuber, H. J.
615   (2019). Impacts of climate change on future air quality and human health in China. *Proceedings of the*
616   *National Academy of Sciences of the United States of America*, *116*(35), 17193–17200.
617   https://doi.org/10.1073/pnas.1812881116

618   Hu, W., Campuzano-Jost, P., Day, D. A., Croteau, P., Canagaratna, M. R., Jayne, J. T., Worsnop, D. R., & Jimenez,
619   J. L. (2017). Evaluation of the new capture vaporizer for aerosol mass spectrometers (AMS) through field
620   studies of inorganic species. *Aerosol Science and Technology*, *51*(6), 735–754.
621   https://doi.org/10.1080/02786826.2017.1296104

622   Indresand, H., White, W. H., Trzepla, K., & Dillner, A. M. (2013). Preparation of sulfur reference materials that
623   reproduce atmospheric particulate matter sample characteristics for XRF calibration. *X-Ray Spectrometry*,
624   *42*(5), 359–367. https://doi.org/10.1002/xrs.2456

625   Jayne, J. T., Leard, D. C., Zhang, X., Davidovits, P., Smith, K. A., Kolb, C. E., & Worsnop, D. R. (2000).
626   Development of an aerosol mass spectrometer for size and composition analysis of submicron particles. In
627   *Aerosol Science and Technology* (Vol. 33, Issues 1–2, pp. 49–70). https://doi.org/10.1080/027868200410840

628   Jimenez, J. L., Jayne, J. T., Shi, Q., Kolb, C. E., Worsnop, D. R., Yourshaw, I., Seinfeld, J. H., Flagan, R. C., Zhang,

629   X., Smith, K. A., Morris, J. W., & Davidovits, P. (2003). Ambient aerosol sampling using the Aerodyne

630   aerosol mass spectrometer. *Journal of Geophysical Research: Atmospheres*, *108*(7).

631   https://doi.org/10.1029/2001jd001213

632 Lalchandani, V., Srivastava, D., Dave, J., Mishra, S., Tripathi, N., Shukla, A. K., Sahu, R., Thamban, N. M.,

633   Gaddamidi, S., Dixit, K., Ganguly, D., Tiwari, S., Srivastava, A. K., Sahu, L., Rastogi, N., Gargava, P., &

634   Tripathi, S. N. (2022). Effect of Biomass Burning on PM2.5 Composition and Secondary Aerosol Formation

635   During Post-Monsoon and Winter Haze Episodes in Delhi. *Journal of Geophysical Research: Atmospheres*,

636   *127*(1), 1–21. https://doi.org/10.1029/2021JD035232

637 Lalchandani, Vipul, Kumar, V., Tobler, A., M. Thamban, N., Mishra, S., Slowik, J. G., Bhattu, D., Rai, P., Satish,

638   R., Ganguly, D., Tiwari, S., Rastogi, N., Tiwari, S., Močnik, G., Prévôt, A. S. H., & Tripathi, S. N. (2021).

639   Real-time characterization and source apportionment of fine particulate matter in the Delhi megacity area

640   during late winter. *Science of the Total Environment*, *770*. https://doi.org/10.1016/j.scitotenv.2021.145324

641 Lipfert, F. W. (1994). Filter artifacts associated with particulate measurements: Recent evidence and effects on

642   statistical relationships. *Atmospheric Environment*, *28*(20), 3233–3249. https://doi.org/10.1016/1352-

643   2310(94)00167-J

644 Makkonen, U., Virkkula, A., Mäntykenttä, J., Hakola, H., Keronen, P., Vakkari, V., & Aalto, P. P. (2012). Semi-

645   continuous gas and inorganic aerosol measurements at a Finnish urban site: Comparisons with filters, nitrogen

646   in aerosol and gas phases, and aerosol acidity. *Atmospheric Chemistry and Physics*, *12*(12), 5617–5631.

647   https://doi.org/10.5194/acp-12-5617-2012

648 Malaguti, A., Mircea, M., La Torretta, T. M. G., Telloli, C., Petralia, E., Stracquadanio, M., & Berico, M. (2015).

649   Comparison of online and offline methods for measuring fine secondary inorganic ions and carbonaceous

650   aerosols in the central mediterranean area. *Aerosol and Air Quality Research*, *15*(7), 2641–2653.

651   https://doi.org/10.4209/aaqr.2015.04.0240

652 Manchanda, C., Kumar, M., Singh, V., Faisal, M., Hazarika, N., Shukla, A., Lalchandani, V., Goel, V., Thamban,

653   N., Ganguly, D., & Tripathi, S. N. (2021). Variation in chemical composition and sources of PM2.5 during the

654   COVID-19 lockdown in Delhi. *Environment International*, *153*(December 2020), 106541.

655   https://doi.org/10.1016/j.envint.2021.106541

656 Minguillón, M. C., Querol, X., Baltensperger, U., & Prévôt, A. S. H. (2012). Fine and coarse PM composition and

657   sources in rural and urban sites in Switzerland: Local or regional pollution? *Science of the Total Environment*,

658   *427–428*, 191–202. https://doi.org/10.1016/j.scitotenv.2012.04.030

659 Nagar, P. K., Singh, D., Sharma, M., Kumar, A., Aneja, V. P., George, M. P., Agarwal, N., & Shukla, S. P. (2017).

660   Characterization of PM2.5 in Delhi: role and impact of secondary aerosol, burning of biomass, and municipal

661   solid waste and crustal matter. *Environmental Science and Pollution Research*, *24*(32), 25179–25189.

662   https://doi.org/10.1007/s11356-017-0171-3

663   Nault, B. A., Campuzano-Jost, P., Day, D. A., Guo, H., Jo, D. S., Handschy, A. V., Pagonis, D., Schroder, J. C.,
664   Schueneman, M. K., Cubison, M. J., Dibb, J. E., Hodzic, A., Hu, W., Palm, B. B., & Jimenez, J. L. (2020).
665   Interferences with aerosol acidity quantification due to gas-phase ammonia uptake onto acidic sulfate filter
666   samples. *Atmospheric Measurement Techniques*, *13*(11), 6193–6213. https://doi.org/10.5194/amt-13-6193-
667   2020

668   Nicolás, J. F., Galindo, N., Yubero, E., Pastor, C., Esclapez, R., & Crespo, J. (2009). Aerosol inorganic ions in a
669   semiarid region on the Southeastern Spanish mediterranean coast. *Water, Air, and Soil Pollution*, *201*(1–4),
670   149–159. https://doi.org/10.1007/s11270-008-9934-2

671   Nie, W., Wang, T., Gao, X., Pathak, R. K., Wang, X., Gao, R., Zhang, Q., Yang, L., & Wang, W. (2010).
672   Comparison among filter-based, impactor-based and continuous techniques for measuring atmospheric fine
673   sulfate and nitrate. *Atmospheric Environment*, *44*(35), 4396–4403.
674   https://doi.org/10.1016/j.atmosenv.2010.07.047

675   Pakkanen, T. A., & Hillamo, R. E. (2002). Comparison of sampling artifacts and ion balances for a Berner low-
676   pressure impactor and a virtual impactor. *Boreal Environment Research*, *7*(2), 129–140.

677   Pandolfi, M., Querol, X., Alastuey, A., Jimenez, J. L., Jorba, O., Day, D., Ortega, A., Cubison, M. J., Comerón, A.,
678   Sicard, M., Mohr, C., Prévôt, A. S. H., Minguillón, M. C., Pey, J., Baldasano, J. M., Burkhart, J. F., Seco, R.,
679   Peñuelas, J., Van Drooge, B. L., … Szidat, S. (2014). Effects of sources and meteorology on particulate matter
680   in the Western Mediterranean Basin: An overview of the DAURE campaign. *Journal of Geophysical
681   Research*, *119*(8), 4978–5010. https://doi.org/10.1002/2013JD021079

682   Pant, P., Shukla, A., Kohl, S. D., Chow, J. C., Watson, J. G., & Harrison, R. M. (2015). Characterization of ambient
683   PM2.5 at a pollution hotspot in New Delhi, India and inference of sources. *Atmospheric Environment*, *109*,
684   178–189. https://doi.org/10.1016/j.atmosenv.2015.02.074

685   Panteliadis, P., Helmink, H. J. P., Koopman, P. C., Hoonhout, M., Jonge, D. De, & Visser, J. H. (2012). *PM 10
686   sampling inlets comparison : EPA vs EU*. *12341*(1999), 12341.

687   Park, S. S., Cho, S. Y., Jo, M. R., Gong, B. J., Park, J. S., & Lee, S. J. (2014). Field evaluation of a near-real time
688   elemental monitor and identification of element sources observed at an air monitoring supersite in Korea.
689   *Atmospheric Pollution Research*, *5*(1), 119–128. https://doi.org/10.5094/APR.2014.015

690   Patel, A., Rastogi, N., Gandhi, U., & Khatri, N. (2021). Oxidative potential of atmospheric PM10 at five different
691   sites of Ahmedabad, a big city in Western India. *Environmental Pollution*, *268*, 115909.
692   https://doi.org/10.1016/j.envpol.2020.115909

693   Pathak, R. K., & Chan, C. K. (2005). Inter-particle and gas-particle interactions in sampling artifacts of PM2.5 in

694 filter-based samplers. *Atmospheric Environment*, *39*(9), 1597–1607.

695 https://doi.org/10.1016/j.atmosenv.2004.10.018

696 Peck, J., Gonzalez, L. A., Williams, L. R., Xu, W., Croteau, P. L., Timko, M. T., Jayne, J. T., Worsnop, D. R.,

697 Miake-Lye, R. C., & Smith, K. A. (2016). Development of an aerosol mass spectrometer lens system for

698 PM2.5. *Aerosol Science and Technology*, *50*(8), 781–789. https://doi.org/10.1080/02786826.2016.1190444

699 Pope, C. A., Ezzati, M., & Dockery, D. W. (2009). Fine-Particulate Air Pollution and Life Expectancy in the United

700 States. *New England Journal of Medicine*, *360*(4), 376–386. https://doi.org/10.1056/nejmsa0805646

701 Querol, X., Pey, J., Minguillón, M. C., Pérez, N., Alastuey, A., Viana, M., Moreno, T., Bernabé, R. M., Blanco, S.,

702 Cárdenas, B., Vega, E., Sosa, G., Escalona, S., Ruiz, H., & Artíñano, B. (2008). PM speciation and sources in

703 Mexico during the MILAGRO-2006 campaign. *Atmospheric Chemistry and Physics*, *8*(1), 111–128.

704 https://doi.org/10.5194/acp-8-111-2008

705 Rai, P., Furger, M., El Haddad, I., Kumar, V., Wang, L., Singh, A., Dixit, K., Bhattu, D., Petit, J. E., Ganguly, D.,

706 Rastogi, N., Baltensperger, U., Tripathi, S. N., Slowik, J. G., & Prévôt, A. S. H. (2020). Real-time

707 measurement and source apportionment of elements in Delhi's atmosphere. *Science of the Total Environment*,

708 *742*. https://doi.org/10.1016/j.scitotenv.2020.140332

709 Rai, P., Slowik, J. G., Furger, M., El Haddad, I., Visser, S., Tong, Y., Singh, A., Wehrle, G., Kumar, V., Tobler, A.

710 K., Bhattu, D., Wang, L., Ganguly, D., Rastogi, N., Huang, R. J., Necki, J., Cao, J., Tripathi, S. N.,

711 Baltensperger, U., & Prevot, A. S. H. (2021). Highly time-resolved measurements of element concentrations

712 in PM10 and PM2.5: Comparison of Delhi, Beijing, London, and Krakow. *Atmospheric Chemistry and*

713 *Physics*, *21*(2), 717–730. https://doi.org/10.5194/acp-21-717-2021

714 Rastogi, N., & Sarin, M. M. (2005). Long-term characterization of ionic species in aerosols from urban and high-

715 altitude sites in western India: Role of mineral dust and anthropogenic sources. *Atmospheric Environment*,

716 *39*(30), 5541–5554. https://doi.org/10.1016/j.atmosenv.2005.06.011

717 Rengarajan, R., Sarin, M. M., & Sudheer, A. K. (2007). Carbonaceous and inorganic species in atmospheric aerosols

718 during wintertime over urban and high-altitude sites in North India. *Journal of Geophysical Research*

719 *Atmospheres*, *112*(21), 1–16. https://doi.org/10.1029/2006JD008150

720 Schaap, M., Spindler, G., Schulz, M., Acker, K., Maenhaut, W., Berner, A., Wieprecht, W., Streit, N., Müller, K.,

721 Brüggemann, E., Chi, X., Putaud, J. P., Hitzenberger, R., Puxbaum, H., Baltensperger, U., & Ten Brink, H.

722 (2004). Artefacts in the sampling of nitrate studied in the "iNTERCOMP" campaigns of EUROTRAC-

723 AEROSOL. *Atmospheric Environment*, *38*(38), 6487–6496. https://doi.org/10.1016/j.atmosenv.2004.08.026

724 Sharma, D., & Kulshrestha, U. C. (2014). Spatial and temporal patterns of air pollutants in rural and urban areas of

725 India. *Environmental Pollution*, *195*(2), 276–281. https://doi.org/10.1016/j.envpol.2014.08.026

726 Sharma, S. K., Mandal, T. K., Jain, S., Saraswati, Sharma, A., & Saxena, M. (2016). Source Apportionment of
727   PM2.5 in Delhi, India Using PMF Model. *Bulletin of Environmental Contamination and Toxicology*, *97*(2),
728   286–293. https://doi.org/10.1007/s00128-016-1836-1

729 Shukla, A. K., Lalchandani, V., Bhattu, D., Dave, J. S., Rai, P., Thamban, N. M., Mishra, S., Gaddamidi, S.,
730   Tripathi, N., Vats, P., Rastogi, N., Sahu, L., Ganguly, D., Kumar, M., Singh, V., Gargava, P., & Tripathi, S. N.
731   (2021). Real-time quantification and source apportionment of fine particulate matter including organics and
732   elements in Delhi during summertime. *Atmospheric Environment*, *261*(July), 118598.
733   https://doi.org/10.1016/j.atmosenv.2021.118598

734 Singh, A., Rastogi, N., Kumar, V., Slowik, J. G., Satish, R., Lalchandani, V., Thamban, N. M., Rai, P., Bhattu, D.,
735   Vats, P., Ganguly, D., Tripathi, S. N., & Prévôt, A. S. H. (2021). Sources and characteristics of light-absorbing
736   fine particulates over Delhi through the synergy of real-time optical and chemical measurements. *Atmospheric*
737   *Environment*, *252*(March). https://doi.org/10.1016/j.atmosenv.2021.118338

738 Singh, A., Satish, R. V., & Rastogi, N. (2019). Characteristics and sources of fine organic aerosol over a big semi-
739   arid urban city of western India using HR-ToF-AMS. *Atmospheric Environment*, *208*(April), 103–112.
740   https://doi.org/10.1016/j.atmosenv.2019.04.009

741 Singhai, A., Habib, G., Raman, R. S., & Gupta, T. (2017). Chemical characterization of PM1.0 aerosol in Delhi and
742   source apportionment using positive matrix factorization. *Environmental Science and Pollution Research*,
743   *24*(1), 445–462. https://doi.org/10.1007/s11356-016-7708-8

744 Takahama, S., Wittig, A. E., Vayenas, D. V., Davidson, C. I., & Pandis, S. N. (2004). Modeling the diurnal variation
745   of nitrate during the Pittsburgh Air Quality Study. *Journal of Geophysical Research D: Atmospheres*, *109*(16).
746   https://doi.org/10.1029/2003JD004149

747 Tobler, A., Bhattu, D., Canonaco, F., Lalchandani, V., Shukla, A., Thamban, N. M., Mishra, S., Srivastava, A. K.,
748   Bisht, D. S., Tiwari, S., Singh, S., Močnik, G., Baltensperger, U., Tripathi, S. N., Slowik, J. G., & Prévôt, A.
749   S. H. (2020). Chemical characterization of PM2.5 and source apportionment of organic aerosol in New Delhi,
750   India. *Science of the Total Environment*, *745*. https://doi.org/10.1016/j.scitotenv.2020.140924

751 Tremper, A. H., Font, A., Priestman, M., Hamad, S. H., Chung, T. C., Pribadi, A., Brown, R. J. C., Goddard, S. L.,
752   Grassineau, N., Petterson, K., Kelly, F. J., & Green, D. C. (2018). Field and laboratory evaluation of a high
753   time resolution x-ray fluorescence instrument for determining the elemental composition of ambient aerosols.
754   *Atmospheric Measurement Techniques*, *11*(6), 3541–3557. https://doi.org/10.5194/amt-11-3541-2018

755 USEPA, & Etv. (2012). *Environmental Technology Verification Report Cooper Environmental Services LLC † Xact*
756   *625 Particulate Metals Monitor*. *September 2012*. http://cooperenvironmental.com/

757 Viana, M., Chi, X., Maenhaut, W., Cafmeyer, J., Querol, X., Alastuey, A., Mikuška, P., & Večeřa, Z. (2006).

758   Influence of sampling artefacts on measured PM, OC, and EC levels in carbonaceous aerosols in an urban

759   area. *Aerosol Science and Technology*, *40*(2), 107–117. https://doi.org/10.1080/02786820500484388

760 Wang, M., Aaron, C. P., Madrigano, J., Hoffman, E. A., Angelini, E., Yang, J., Laine, A., Vetterli, T. M., Kinney, P.

761   L., Sampson, P. D., Sheppard, L. E., Szpiro, A. A., Adar, S. D., Kirwa, K., Smith, B., Lederer, D. J., Diez-

762   Roux, A. V., Vedal, S., Kaufman, J. D., & Barr, R. G. (2019). Association between long-term exposure to

763   ambient air pollution and change in quantitatively assessed emphysema and lung function. *JAMA - Journal of*

764   *the American Medical Association*, *322*(6), 546–556. https://doi.org/10.1001/jama.2019.10255

765 Wu, W. S., & Wang, T. (2007). On the performance of a semi-continuous PM2.5 sulphate and nitrate instrument

766   under high loadings of particulate and sulphur dioxide. *Atmospheric Environment*, *41*(26), 5442–5451.

767   https://doi.org/10.1016/j.atmosenv.2007.02.025

768 Zhang, D., Shi, G. Y., Iwasaka, Y., & Hu, M. (2000). Mixture of sulfate and nitrate in coastal atmospheric aerosols:

769   Individual particle studies in Qingdao (36°04'N, 120°21'E), China. *Atmospheric Environment*, *34*(17), 2669–

770   2679. https://doi.org/10.1016/S1352-2310(00)00078-9

771 Zhang, X., & Mcmurryt, P. H. (1992). EVAPORATIVE LOSSES OF FINE PARTICULATE NITRATES DURING

772   SAMPLING. In *Atmospheric Environment* (Vol. 26, Issue 18).

773